Low Energy Quantum Scattering in Waveguides

A thesis presented

by

Andy Itsara

to

The Department of Physics

in partial fulfillment of the requirements

for the degree of

Bachelor of Arts

in the subject of

Chemistry and Physics

Harvard University

Cambridge, Massachusetts

May, 2005

Contents

Chapter 1

Introduction and Outline of the Thesis

1.1 Introduction

Scattering off of impurities in waveguides has been a topic of considerable interest in both experiment and theory. In the late 1980s with exhibition of quantized conduction in confining potentials, the study of impurities was of interest for their role in reduction of conductance in GaAs/AlGaAs heterostructures [6, 8, 27].

More recently, the effect of impurities on electron flow has been of a topic interest with an eye towards mesoscopic devices [26]. In addition to GaAs/GaAlAs heterostructures, carbon nanotubes have also been demonstrated to act as few-mode quantum waveguides [16]. Coherence of atoms through waveguides are expected to play an important role in such devices as atomic interferometry and quantum computing and thus have been a subject of theoretical interest [20].

Using results from low-energy and multiple scattering, most notably "renormalized t-matrix" theory as developed by A. Lupu-Sax [18], we present in this thesis a theory of scattering in waveguides. While we primarily focus on s-wave scattering through the use of zero range interactions, we also derive an optical theorem for a two-dimensional waveguide geometry. Finally, we interpret our results for the cross section and conductance due to a scattering impurity in the context of multiple-scattering,

1.2 Outline of the Thesis

In chapter 2 we begin by highlighting concepts from elementary quantum mechanics that will be of key importance in two-dimensional scattering: free particles in both the plane and cylindrical wave basis, probability flux and its continuity, and normalization to unit flux, which will be of key importance when we look at scattering in waveguides. This material may be found in most, if not all standard texts; we attempt a presentation tailored to the essentials needed to approach scattering theory.

In chapter 3 we continue our review of quantum mechanics with a development of scattering in free space. As we will eventually consider two-dimensional scattering, our treatment differs from the traditional in that we will focus on two as opposed to three dimensions. As with traditional treatments, we cover the Lippman-Schwinger equation and Green's functions as well as Born Approximation and Partial Wave Analysis. Finally, we derive an optical theorem in two dimensions and introduce the S matrix.

Low energy scattering is well-discussed in standard texts and indeed continues to be a topic of great interest in the literature [13, 7, 21, 12]. In chapter 4, we briefly review the importance of s-wave scattering in the low energy limit and proceed to introduce the s-wave Point Scatterer Model discussing some of its applications to free space scattering. Having discussed the single scatterer case for sometime, we then proceed to develop multiple scattering theory, with an emphasis on its relation to the s-wave point scatterer model as well as its more general application in so-called "renormalized t-matrix" theory.

In chapter 5, all the concepts we have discussed in scattering theory are brought together in formulation of scattering theory for a waveguide. For simplicity, when we need to be more specific, we focus on a waveguide whose transverse confinement potential consists of two infinitely hard walls a distance W apart.

We begin with a fairly unconventional approach to calculation of the Green's function making use of the method of images. We then proceed to translate the concept of scattering strength of a point scatterer in free space to the same potential in the wire making use of renormalized t-matrices as developed in the previous chapter. Continuing our development of the s-wave Point Scatterer Model in the wire, we then develop a concept of the cross-section, the S-matrix, and a point scatterer "optical theorem" for a waveguide.

Having developed a means of modeling s-wave scattering in a waveguide, we exhibit various scattering phenomena in the waveguide including proximity resonances, cross-section behavior near threshold energies, and its effect on conductance through the wire.

Finally, conclude the chapter by developing an optical theorem for general potentials in the wire, making note of its similarities to both the one- and two-dimensional free space optical theorems. For the special case of a point scatterer scattering the $m = 0$ wave of a periodic wire, we demonstrate in the wide waveguide limit that the waveguide optical theorem degenerates to the two-dimensional free space one.

In chapter 6, we present some conclusions and ideas for future directions of this work. This is followed by appendices containing formulas for reference and some of the more involved mathematical calculations referred to in the thesis.

Chapter 2

A Review of Free Space Wave Functions

In quantum scattering, the incoming wave is usually assumed to be freely propagating in space before interacting with a scattering potential, and once again propagating freely away from the scatterer. We present in this chapter particularly relevant concepts in two-dimensional quantum mechanics that are used in scattering theory. We begin with a review free particles in quantum mechanics in both the plane wave $|p\rangle$ and the 2D-cylindrical wave $|E, m\rangle$ bases. As the optical theorem and waveguide scattering will be discussed in later chapters, we also review probability flux in quantum mechanics.

2.1 Free Particles

2.1.1 Plane Waves

In free space, the Hamiltonian is just the kinetic energy operator. In Cartesian coordinates this is

$$\hat{H} = \frac{\hat{p}^2}{2m} = -\frac{\hbar^2}{2m}\nabla^2$$

so that the time-independent Schrodinger equation is simply

$$\frac{\hat{p}^2}{2m}\psi = E\psi \tag{2.1}$$

Switching into ket notation, we have that

$$H|p\rangle = \frac{p^2}{2m}|p\rangle$$

Since [H,p] = 0, we can characterize our states by momentum choosing $|p\rangle$ as our eigenkets for H. If we want to put our kets in the x-basis, then we have to solve the differential equation

$$\frac{\hat{p}^2}{2m}\psi = E\psi \tag{2.2}$$

$$\Rightarrow \frac{-\hbar^2}{2m}\nabla^2\psi = E\psi \tag{2.3}$$

$$\Rightarrow \nabla^2\psi - \frac{2mE}{\hbar^2}\psi = 0 \tag{2.4}$$

This is a familiar differential equation with solution $\psi = Ae^{i\mathbf{k}\cdot\mathbf{x}}$ where $\mathbf{k} \equiv (\mathbf{k_x}, \mathbf{k_y}, \mathbf{k_z})$ subject to the constraint that $\sum k_i^2 = \frac{2mE}{\hbar^2}$. Applying the momentum operator, we find that $p = \hbar|\mathbf{k}|$ for the magnitude of the momentum. The overall solution to the Schrodinger equation is just

$$\langle \mathbf{x}|\mathbf{p}\rangle = \mathbf{A}\mathbf{e}^{\mathbf{ik}\cdot\mathbf{x}-\mathbf{i}\omega\mathbf{t}} \tag{2.5}$$

The constant A is determined by the chosen normalization condition to be imposed. The ω term is determined in general for any solution of the time-independent Schrodinger equation of a system to be $\omega = \frac{E}{\hbar}$. For the case of the free particle, we have the additional relations

$$\omega = \frac{E}{\hbar} = \frac{\mathbf{p^2}}{2m\hbar} = \frac{\hbar\mathbf{k^2}}{2m} \tag{2.6}$$

Normalization into an orthonormal complete set is determined by requiring that

$$\langle p'|p\rangle = \delta(p'-p)$$

Recall from classical mechanics that if we have a function $f(t)$, we can define its Fourier transform in frequency space $F(\omega)$ and its inverse by

$$F(\omega) = \int_{-\infty}^{\infty} f(t)e^{i\omega t}\ \mathrm{d}t \tag{2.7}$$

$$f(t) = \frac{1}{2\pi}\int_{-\infty}^{\infty} F(\omega)e^{-i\omega t}\ \mathrm{d}\omega \tag{2.8}$$

Since $\psi(x) = \langle x|p\rangle = Ae^{ikx}$, we see that position and momentum eigenkets satisfy a similar relationship in quantum mechanics

$$\psi(x) = \langle x|\psi\rangle = \int \langle x|k\rangle\langle k|\psi\rangle dk = \frac{1}{\sqrt{2\pi}}\int_{-\infty}^{\infty} e^{ikx}\langle k|\psi\rangle dk \tag{2.9}$$

$$\psi(k) = \langle k|\psi\rangle = \int \langle k|x\rangle\langle x|\psi\rangle dx = \frac{1}{\sqrt{2\pi}}\int_{-\infty}^{\infty} e^{-ikx}\langle x|\psi\rangle dx \tag{2.10}$$

$$\tag{2.11}$$

Here we are using $k \equiv \frac{p}{\hbar}$. The factor $\frac{1}{\sqrt{2\pi}}$ arises in both terms here but not in the former case because the substitution $\omega = 2\pi\nu$ has been used for the classical case. From inspecting (2.9) and (2.10), we see in the one-dimensional case, $\langle x|p\rangle = \frac{1}{\sqrt{2\pi}}e^{i(kx-\omega t)}$ and that

$$\langle x|x'\rangle \equiv \delta(x-x') = \int \langle x|p\rangle\langle p|x'\rangle dp = \frac{1}{2\pi}\int_{-\infty}^{\infty} e^{ik(x-x')}dk$$

More generally, $A = \frac{1}{(2\pi)^{\frac{d}{2}}}$, where d is the dimension in which the waves are propagating. Thus the general form of a plane wave of specified momentum in d-dimensions is simply

$$\langle x|k\rangle = \psi_k(x,t) = \frac{1}{(2\pi)^{\frac{d}{2}}}e^{\mathbf{ik}\cdot\mathbf{x}-\mathbf{i}\omega\mathbf{t}} \tag{2.12}$$

Later, we will derive another normalization of by requiring unit flux through a given area, a relevant quantity when considering particle transport through a waveguide.

2.1.2 Cylindrical Waves

In two-dimensions, we may further classify a free particle not only by its energy, but its angular momentum as well. This will become relevant when we consider scattering by some localized potential. While viewing an incoming wave is naturally done in Cartesion coordinates, the scattered wave is more easily treated according to its relative direction of propagation relative to the incoming wave, and thus polar coordinates are of great use.

The angular momentum operator L_z is defined in polar coordinates by

$$\hat{L}_z = -i\hbar\frac{\partial}{\partial\phi} \tag{2.13}$$

The eigenfunctions to this are simply of the form $e^{im\phi}$ with eigenvalues $m\hbar$, $m \in \mathbb{Z}$. In polar coordinates and for a radially symmetric potential, the Schrodinger Equation $H\psi = E\psi$ becomes

$$\{-\frac{\hbar^2}{2\mu}(\frac{\partial^2}{\partial r^2} + \frac{1}{r}\frac{\partial}{\partial r} + \frac{1}{r^2}\frac{\partial^2}{\partial\phi^2}) + V(r)\}\psi(r,\phi) = E\psi(r,\phi) \tag{2.14}$$

$$\Rightarrow \{-\frac{\hbar^2}{2\mu}(\frac{\partial^2}{\partial r^2} + \frac{1}{r}\frac{\partial}{\partial r} - \frac{1}{r^2}\frac{L_z^2}{\hbar^2}) + V(r)\}\psi(r,\phi) = E\psi(r,\phi) \tag{2.15}$$

It is clear by inspection that [H, L_z] = 0 and thus we may define simultaneous eigenkets $|E,m\rangle$. Using separation of variables with $\psi(r,\phi) = R(r)\Phi(\phi)$, we find that $\psi(r,\phi) = R(r)e^{im\phi}$. For a free particle, the radial equation becomes

$$\{-\frac{\hbar^2}{2\mu}(\frac{\partial^2}{\partial r^2} + \frac{1}{r}\frac{\partial}{\partial r} - \frac{m^2}{r^2})\}R(r) = ER(r) \tag{2.16}$$

Under the substitution $u = kr = \sqrt{\frac{2\mu E}{\hbar^2}}r$ and subsequent multiplication by u^2, this equation becomes

$$[u^2\frac{\partial^2}{\partial u^2} + u\frac{\partial}{\partial u} + (u^2 - m^2)]R(u) = 0 \tag{2.17}$$

The solutions to this equation are the Bessel Functions of the First and Second Kind, denoted by $J_m(kr)$ and $Y_m(kr)$, respectively. Bessel functions of the second kind $Y_m(kr)$ are singular at the origin and thus contribute only to either to potentials that are singular at the origin or solutions of problems away from the origin. For a free particle then, we only use the $J_m(kr)$ solutions. For normalization, we have the property that

$$\langle E', m'|E, m\rangle = \int e^{i(m'-m)\phi} \int rJ_m(k'r)J_m(kr)\ \mathrm{d}r\ \mathrm{d}\phi = \frac{2\pi}{k}\delta_{m'm}\delta(E'-E)$$

so that our normalization constant is $C_{k,m} = \sqrt{\frac{k}{2\pi}}$. The final form for the $|E,m\rangle$ basis is

$$\langle x|E,m\rangle = \sqrt{\frac{k}{2\pi}}J_m(kr)e^{im\phi/\hbar} \tag{2.18}$$

To relate plane waves to spherical waves, we have the Jacobi-Anger expansion of a plane wave:

$$\frac{e^{ik\cdot r}}{2\pi} = \frac{e^{ikr\cos\phi}}{2\pi} = \frac{1}{2\pi}\sum_{n=-\infty}^{\infty} i^n J_n(kr)e^{in\phi} \tag{2.19}$$

Finally, cylindrical waves away from the origin are often expressed as a linear combination of the Bessel functions known as the Hankel functions of the first and second kind:

$$H_l^{(1)}(kr) \equiv J_l(kr) + iY_l(kr) \tag{2.20}$$

$$H_l^{(2)}(kr) \equiv J_l(kr) - iY_l(kr) \tag{2.21}$$

Further properties of these functions are listed in Appendix D.

2.2 Flux and Normalization

2.2.1 Continuity of Flux

From classical physics, we know that in the world of electromagnetism, the total charge is conserved and that it flows in a continuously. Alternately, in statistical mechanics, we also have particle conservation and continuous flow. In both cases, this is expressed in the differential relation

$$\frac{\partial}{\partial t}\rho(\vec{r},t) = -\nabla\cdot\mathbf{j} \tag{2.22}$$

In words, the local rate of change in charge (particle) density is equal to the net in or outward flow of charge density in the unit area of interest; there are no charge (particle) destroying or creating sources. On the global, level an equivalent statement is

$$\frac{\partial}{\partial t}\int_V d^3r\rho(\vec{r},t) = -\int_V d^3r\nabla\cdot\mathbf{j} = -\int_{\partial V} j\cdot dS \tag{2.23}$$

Now a quantum system has an analogous concept. For a QM system, we know that

$$\langle\psi(0)|\psi(0)\rangle = \langle\psi(t)|\psi(t)\rangle$$

which is to say that the total probability of finding a particle is conserved. Now

$$\langle\psi(t)|\psi(t)\rangle = \int d\tau\psi^*\psi \equiv \int d\tau P(r,t) = \text{const.}$$

so that as we have defined, we may consider $P(r,t)$, the probability density to be a conserved quantity. Using the Schrodinger equation, we have that

$$i\hbar\frac{\partial}{\partial t}\psi = -\frac{\hbar^2}{2m}\nabla^2\psi + V\psi$$

and another equation if we take its conjugate. Through an appropriate combination of the two equations, we get that

$$\begin{aligned} i\hbar\frac{\partial}{\partial t}(\psi^*\psi) &= -\frac{\hbar^2}{2m}(\psi^*\nabla^2\psi - \psi\nabla^2\psi^*) && (2.24)\\ \Rightarrow \frac{\partial}{\partial t}P &= -\frac{\hbar}{2mi}\nabla\cdot(\psi^*\nabla\psi - \psi\nabla\psi^*) && (2.25)\\ \Rightarrow \frac{\partial}{\partial t}P &= -\nabla\cdot j && (2.26)\end{aligned}$$

where we have defined $j \equiv \frac{\hbar}{2mi}(\psi^*\nabla\psi - \psi\nabla\psi^*) = \frac{\hbar}{m}\text{Im }(\psi^*\nabla\psi)$. As the classical case interpreted j as the charge current density, in the quantum analogue, we see the it takes on meaning as the probability current density.

2.2.2 Normalization to Unit Flux

For a waveguide, the relevant quantity in normalization of a wavefunction propagating through the system is not normalization to a Dirac-delta function, but rather to unit flux moving through the system. For a plane wave $\psi = Ae^{i\vec{k}\cdot\vec{x}}$, the flux in some direction $\hat{v}$ is given by

$$\begin{aligned} \hat{v}\cdot\vec{j} &= \hat{v}\cdot(\frac{\hbar}{m}\text{Im }(\psi^*\nabla\psi)) && (2.27)\\ &= \hat{v}\cdot(|A|^2\sum k_i) && (2.28)\\ &= |k||A|^2\cos\phi && (2.29)\end{aligned}$$

where ϕ is the angle between the vector $\vec{k}$ an $\hat{v}$. For $\phi = 0$, normalization to unit flux per unit length, area, or volume yields

$$\psi = \frac{e^{ik \cdot x}}{\sqrt{k}} \tag{2.30}$$

a useful basis when deriving quantities such as conductance. However eigenfunction expansion using this basis at some energy $E = \frac{\hbar^2 k^2}{2\mu}$ now takes on the somewhat inconvenient form

$$\int d\Omega |k\rangle\langle k| = \frac{(2\pi)^2}{k} \tag{2.31}$$

so that often it is best to move between these normalization to flux and normalization to a delta function.

Chapter 3

Scattering Theory in Two Dimensions

In this chapter, we review the key concepts of scattering theory including the Green's Function, partial wave analysis, phase shifts, and the optical theorem. Because we will be considering waveguide scattering in two dimensions, we will focus on two-dimensions here as well. Treatments of three-dimensional scattering may be found in several standard texts including [22] and [23].

3.1 Integral Form of the Schrodinger Equation

Because the incoming wavefunction is usually considered to be a free particle, the Hamiltonian for the system is often labeled as

$$H = H_0 + V \tag{3.1}$$

where H_0 represents the Hamiltonian of a free particle, $H_0 = \frac{\boldsymbol{p}^2}{2m}$, which is just the kinetic energy operator, and V represents the scattering potential. More generally, H_0 can represent the Hamiltonian of a "background" potential while V is the scattering potential in the presence of the background. We assume elastic scattering so that given $H_0|\phi\rangle = E|\phi\rangle$, we look for solutions satisfying $H|\psi\rangle = (H_0 + V)|\psi\rangle = E|\psi\rangle$. We also assume that as V $\to 0$, $\psi \to \phi$.

Now through algebraic manipulation of (3.1), we have that

$$\begin{aligned} (H_0 + V)|\psi\rangle &= |\psi\rangle & (3.2)\\ \Rightarrow (E - H_0)|\psi\rangle &= V|\psi\rangle + 0 & (3.3)\\ \Rightarrow (E - H_0)|\psi\rangle &= V|\psi\rangle + (E - H_0)|\phi\rangle & (3.4)\\ \Rightarrow |\psi\rangle &= \frac{1}{E - H_0} V|\psi\rangle + |\phi\rangle & (3.5) \end{aligned}$$

so that (3.5) seems to work aside from the singularities when ψ is an eigenfunction of H. To avoid this singularity, (3.5) is made slightly complex

$$|\psi^{\pm}\rangle = \frac{1}{E - H_0 \pm i\epsilon} V|\psi^{\pm}\rangle + |\phi\rangle \tag{3.6}$$

and thus we have in equation (3.6) the Lippman-Schwinger equation. The physical meaning of $\pm$ will turn out to correspond to outgoing and incoming scattered waves, respectively so we will deal with the ψ^+ solutions. Unfortunately, the Lippmann-Schwinger equation has not reduced the amount of work needed to solve for ψ. After all, ψ appears on both sides of the equation. If we write this in the position basis, (expand via $\langle x|$), we have that

$$\begin{aligned} \langle x|\psi^{\pm}\rangle &= \langle x|\phi\rangle + \int d^2x' \langle x|\frac{1}{E - H_0 \pm i\epsilon}|x'\rangle\langle x'|V|\psi^{\pm}\rangle & (3.7)\\ \Rightarrow \psi^+(x) &= \phi(x) + \int d^2x' \langle x|\frac{1}{E - H_0 + i\epsilon}|x'\rangle V(x')\psi^+(x') & (3.8) \end{aligned}$$

so that solving a differential equation has been transformed into solving an integral equation. This form of the Schrodinger equation consequently lends itself to various approximation techniques to solutions of the scattering problem.

3.2 Green's Functions

The kernel of the integral in (3.8), $\langle x|\frac{1}{E-H_0+i\epsilon}|x'\rangle$ understandably plays a key role in solutions of the system. For this reason, the operator

$$G \equiv \frac{\hbar^2}{2\mu}\langle x|\frac{1}{E-H_0+i\epsilon}|x'\rangle \tag{3.9}$$

is defined as the Green's operator with $\langle x|G|x\rangle = G(x,x')$ known as the Green's function of the system. Actually, we are using one of two commonly used conventions for the Green operator and function here. The convention used here defines the Green's function, as we will soon see, to be the solution to a differential equation free of any quantum mechanical constants. Other texts define $\langle x|\frac{1}{E-H_0+i\epsilon}|x'\rangle$ itself as the Green's operator for convenience in operator manipulation. The choice of convention is up to personal preference and in any case, does not affect any of the derivations to follow aside from the removal or insertion of a constant. If we apply $\langle x|(E-H_0)$ to equation (3.6), we have that

$$\langle x|V|\psi\rangle = \frac{2\mu}{\hbar^2}\langle x|(E-H_0)GV|\psi\rangle + 0 \tag{3.10}$$

$$\langle x|V|\psi\rangle = \frac{2\mu}{\hbar^2}\int d^2x'\langle x|(E-H_0)G|x'\rangle\langle x'|V|\psi\rangle \tag{3.11}$$

$$\Rightarrow \frac{2\mu}{\hbar^2}\langle x|(E-H_0)G|x'\rangle = \langle x|x'\rangle = \delta^{(2)}(x-x') \tag{3.12}$$

For a two-dimensional free-space system, $H_0 = -\frac{\hbar^2}{2\mu}\nabla^2$ and writing $E = \frac{\hbar^2k^2}{2\mu}$, equation (3.12) in x-coordinates is just the differential equation

$$(\nabla^2 + k^2)G(x,x';k) = \delta^{(2)}(x-x') \tag{3.13}$$

There are various methods of solving for the Green's function of a system $G(r,r';k)$, but for brevity, we state here the result for the Green's function for $H_0 = \frac{\hat{p}^2}{2\mu}$, the two-dimensional free particle Green's function.

$$G^+(r,r';k) = -\frac{i}{4}H_0^{(1)}(k|r-r'|) \tag{3.14}$$

where $k = \sqrt{\frac{2\mu E}{\hbar^2}}$. Here, $H_0^{(1)}(k|r-r'|)$ refers to the Hankel function of the first kind $H_l^{(1)}(x) = J_l(x) + iY_l(x)$ mentioned in Section 2.1.2. Because of translational symmetry, it is natural to express the Green's function in polar coordinates as only a function of $\rho = |r-r'|$. In this case, it satisfies the equation

$$(\nabla^2 + k^2)G(|\rho-\rho'|;k) = \delta(r-r') \equiv \frac{1}{2\pi\rho}\delta(\rho)$$

3.3 Born Approximation

We now discuss the use of the Born approximation in solving equation (3.8). The obstacle to finding an analytic solution to the equation is the appearance of the final wavefunction ψ^+ itself on both sides of the equation. For the case of weak scattering is relatively weak, then at times it can be reasonable to approximate within the integral that $\psi^{(+)}(x) \approx \phi(x)$. Making this approximation allows us to solve for the final wavefunction ψ^+. This is known as the first Born approximation:

$$\psi^+(x) \approx \phi(x) + \frac{2\mu}{\hbar^2}\int d^2x'\langle x|G|x'\rangle V(x')\phi(x') \tag{3.15}$$

More generally, we want to construct a better series of approximations in the spirit of the first-order Born approximation. We define the operator T to satisfy the relation

$$V|\psi\rangle = T|\phi\rangle \tag{3.16}$$

Clearly knowing the T operator would be equivalent to solving the scattering problem as we would have that $\psi = (1 + \frac{2\mu}{\hbar^2}GT)\phi$. However, as it is usually not analytically possible, we instead derive a recursive relation for it by applying V to both sides of (3.6) to get

$$\begin{aligned} V|\psi\rangle = T|\phi\rangle &= V|\phi\rangle + V(\frac{2\mu}{\hbar^2}G)V|\psi\rangle & (3.17) \\ &= V|\phi\rangle + V(\frac{2\mu}{\hbar^2}G)T|\phi\rangle & (3.18) \end{aligned}$$

which tells us that the T operator satisfies the recursive relation

$$T = V + V(\frac{2\mu}{\hbar^2}G)T \tag{3.19}$$

that we can iterate the relation (3.19) to get the Born series

$$T = V + V(\frac{2\mu}{\hbar^2}G)V + V(\frac{2\mu}{\hbar^2}G)V(\frac{2\mu}{\hbar^2}G)V + \ldots \tag{3.20}$$

or formally solve to get

$$T = (1 - V(\frac{2\mu}{\hbar^2}G))^{-1}V = V(1 - (\frac{2\mu}{\hbar^2}G)V)^{-1} \tag{3.21}$$

Convergence issues aside, equation (3.20) thus tells us that one may solve for the scattering solution through an infinite series of integrals. Successive approximations may be carried out by truncating the Born series. Alternately, representation of T as in equation (3.21) is a good mnemonic device and a useful form for formal manipulations in relation to other operators as we will see in our discussion of renormalized t-matrices in section 4.6.

3.4 Asymptotic Form of Scattered Waves

At very large distances from the effective range of the scatterer, the wavefunction takes on a certain form independent of potential. The asymptotic form of the scattered wavefunction will play a key part in our discussion of the optical theorem and flux conservation. In addition, it is at these distances that many experimental observations occur. Substituting in two dimensions into equation (3.8), we have the general solution for a scattering problem in two-dimensions:

$$\psi^+(x) = \phi(x) + \frac{2\mu}{\hbar^2}\int d^2x' G_0(k|x - x'|)\langle x'|V|\psi^+\rangle \tag{3.22}$$

Now we want to take the limit when we're observing at x very far away from the scatterer, so that for practical purposes, the scatterer acts on a finite range and the point of observation is far from this range. Taking the origin to be the center of the scatter, we introduce some variables: $r = |\vec{x}|$, $r' = |\vec{x'}|$, and α the angle between the two points. Then for $r \gg r'$, we can approximate the argument $|x - x'|$ as follows

$$\begin{aligned} |\vec{x} - \vec{x'}| &= \sqrt{r^2 - 2rr'\cos\alpha + r'^2} & (3.23) \\ &= r\sqrt{1 - \frac{2r'}{r}\cos\alpha + \frac{r'^2}{r^2}} & (3.24) \\ &\approx r\sqrt{1 - \frac{2r'}{r}\cos\alpha} \approx r(1 - \frac{r'}{r}\cos\alpha) & (3.25) \\ &\approx r - r'\cos\alpha = r - \hat{x}\cdot\vec{x'} & (3.26) \end{aligned}$$

At large x, we can also take the asymptotic form of the Green's function:

$$G_0(k|x-x'|) = -\frac{i}{4}H_0^{(1)}(k|x-x'|) \to -\frac{i}{4}\sqrt{\frac{2}{\pi}}e^{-i\pi/4}\frac{e^{ik|x-x'|}}{\sqrt{|x-x'|}} \approx -\frac{1}{4}\sqrt{\frac{2}{\pi}}e^{i\pi/4}\frac{e^{ik|x-x'|}}{\sqrt{k|x|}} \tag{3.27}$$

Combining this with our earlier approximation of the argument $|x-x'|$,

$$\frac{e^{ik|x-x'|}}{\sqrt{k|x|}} \approx \frac{e^{ikr}}{\sqrt{r}}\frac{e^{-ik\hat{x}\cdot x'}}{\sqrt{k}} \tag{3.28}$$

we may rewrite equation (3.22) as

$$\psi^+(x) = \phi(x) + \frac{e^{ikr}}{\sqrt{r}}[-\frac{\mu}{2\hbar^2}\sqrt{\frac{2}{k\pi}}e^{i\pi/4}\int d^2x' e^{-ik\hat{x}\cdot x'}\langle x'|V|\psi^+\rangle] \tag{3.29}$$

$$= \phi(x) + \frac{e^{ikr}}{\sqrt{r}}[-\frac{\mu}{2\hbar^2}\sqrt{\frac{2}{k\pi}}e^{i\pi/4}\langle k'|V|\psi^+\rangle]] \tag{3.30}$$

$$= \phi(x) + \frac{e^{ikr}}{\sqrt{r}}f(k,k') \tag{3.31}$$

where in equation (3.30) we have defined $k' \equiv k\hat{x}$, a vector of magnitude k pointing from the origin to the point x, and $\langle k'|\vec{x}\rangle$ the unnormalized plane-wave $e^{-ik'r}$. In equation (3.31), we have defined

$$f(k,k') \equiv -\frac{\mu}{\hbar^2}\sqrt{\frac{1}{2\pi k}}e^{i\pi/4}\langle k'|V|\psi^+\rangle \tag{3.32}$$

Asymptotically, the term $\frac{e^{\pm ikr}}{\sqrt{kr}}$ pulls out of the integral. This term represents free propagation of the wave moving away from the scatterer which is intuitively expected if the wave is no longer interacting with the scatterer. Equation (3.31) demonstrates that the scattering amplitude in a particular direction, $f(k,k')$ depends on the energy, angle, and incoming wave.

3.5 The Scattering Amplitude f(k,k')

While equation (3.31) may be more physically intuitive, the challenge still remains in calculating $f(k,k') = \langle k'|T|\phi\rangle$. It is here that the Born Series is applied to create a series of functions $f^{(n)}(k,k')$ whose sum is $f(k,k')$.

$$f(k,k') = \sum_{n=1}^{\infty} f^{(n)}(k,k') \tag{3.33}$$

where

$$f^{(n)}(k,k') = -\frac{\mu}{\hbar^2}\sqrt{\frac{1}{2\pi k}}e^{i\pi/4}\langle k'|V(\frac{2\mu}{\hbar^2}GV)^{n-1}|\phi\rangle \tag{3.34}$$

The function $|f(k,k')|^2$ also takes on significant physical meaning. Classically, we can imagine sending in a wave to bombard some hard object and having some of the wave scatter. Then measuring the total scattered flux and dividing by the incoming flux per unit area would yield the cross-section seen by the incoming wave

$$\frac{\text{(scattered flux)}}{\text{(incoming flux) / area}} = \text{area}$$

We define the differential cross-section $\frac{d\sigma}{d\theta}$ similarly as the scattered flux into solid angle $d\theta$ per unit incident flux of the plane wave:

$$\frac{d\sigma}{d\theta} = \frac{r|j_{\text{scat}}|}{|j_{\text{inc}}|} \tag{3.35}$$

Taking $\phi(x) = e^{ikx}$ in equation (3.31), we find that

$$j_{\text{scat}} = \frac{\mu}{\hbar}\text{Im }(\psi^*_{\text{scat}}\nabla\psi_{\text{scat}}) = \text{Im }(-\frac{1}{2r^2} + \frac{ik}{r}) \quad = \quad \frac{\mu k}{\hbar r} \tag{3.36}$$

$$j_{\text{inc}} = \frac{\mu}{\hbar}\text{Im }(\psi^*_{\text{inc}}\nabla\psi_{\text{inc}}) = \text{Im }(ik) \quad = \quad \frac{\mu k}{\hbar} \tag{3.37}$$

$$\Rightarrow \frac{d\sigma}{d\theta} \quad = \quad |f(k,k')|^2 \tag{3.38}$$

so as in the three-dimensional case, $|f(k,k')|^2$ is exactly the differential cross-section.

3.6 Partial Wave Analysis

With the asymptotic from of the 2D scattered wave (3.31) and the expansion of a plane wave as cylindrical waves in (2.19), it becomes natural to put the entire asymptotic scattering solution in terms of the $|E, m\rangle$ basis functions. Away from the origin, the Bessel functions of the second kind, $Y_m(kr)$ become feasible solutions to the scattered wave and it will be convenient to write our scattered wave in terms of the Hankel functions $H_l^{(1)}(kr)$ and $H_l^{(2)}(kr)$. As seen in Appendix D.2, our basis functions asymptotically become

$$H_m^{(1)}(kr)e^{im\phi} \to \sqrt{\frac{2}{\pi kr}}e^{i(kr - m\pi/2 - \pi/4)}e^{im\phi} \tag{3.39}$$

$$H_m^{(2)}(kr)e^{im\phi} \to \sqrt{\frac{2}{\pi kr}}e^{-i(kr - m\pi/2 - \pi/4)}e^{im\phi} \tag{3.40}$$

where for now, the normalization constant $\sqrt{\frac{k}{2\pi}}$ has been ignored. Equation (2.19) now asymptotically takes on the form

$$e^{ik\cdot r} \quad = \quad \sum_{m=-\infty}^{\infty} i^m J_m(kr)e^{im\phi} \tag{3.41}$$

$$= \quad \sum_{m=-\infty}^{\infty} i^m (\frac{H_m^{(1)}(kr) + H_m^{(2)}(kr)}{2})e^{im\phi} \tag{3.42}$$

$$= \quad \sum_{m=-\infty}^{\infty} i^m (\frac{H_m^{(1)}(kr) + H_m^{(2)}(kr)}{2})e^{im\phi} \tag{3.43}$$

$$\to \quad \sum_{m=-\infty}^{\infty} \sqrt{\frac{1}{2\pi kr}} i^m (e^{i(kr - m\pi/2 - \pi/4)} + e^{-i(kr - m\pi/2 - \pi/4)})e^{im\phi} \tag{3.44}$$

$$= \quad \sum_{m=-\infty}^{\infty} \sqrt{\frac{1}{2\pi kr}} (e^{i(kr - \pi/4)} + e^{-i(kr - m\pi - \pi/4)})e^{im\phi} \tag{3.45}$$

Similarly, we expand the scattered wave into cylindrical basis functions by expanding $f(\phi) \propto \langle k'|V|\psi^+\rangle$ in terms of the L_z basis functions $e^{im\phi}$:

$$\psi_{\text{scat}} \quad = \quad f(\phi)\frac{e^{ikr}}{\sqrt{r}} \tag{3.46}$$

$$= \quad (\sum_{m=-\infty}^{\infty} f_m e^{im\phi})\frac{e^{ikr}}{\sqrt{r}} \tag{3.47}$$

$$= \quad \sum_{m=-\infty}^{\infty} (f_m e^{i\pi/4}\sqrt{2\pi k})\sqrt{\frac{1}{2\pi kr}}e^{i(kr - \pi/4)}e^{im\phi} \tag{3.48}$$

Combining equations (3.45) and (3.48) to get the final wavefunction, we have that

$$\psi = \sqrt{\frac{1}{2\pi kr}} \sum_{m=-\infty}^{\infty} ((1 + f_m e^{i\pi/4}\sqrt{2\pi k})e^{i(kr-\pi/4)} + e^{-i(kr-m\pi-\pi/4)})e^{im\phi} \tag{3.49}$$

which may be written as

$$\psi = \sum_{m=-\infty}^{\infty} \left(\frac{e^{2i\delta_l}}{2} H_l^{(1)}(kr) + \frac{1}{2} H_l^{(2)}(kr) \right) e^{il\phi} e^{il\pi/2} \tag{3.50}$$

Thus the incoming plane-wave has been written as the sum of incoming and outgoing cylindrical waves. After scattering, only the outgoing wave has been affected by a phase shift.

Because we are looking at a time-independent problem, it must be that the incoming flux is the same as the outgoing flux. Furthermore, because angular momentum is conserved, it must be that flux conservation holds for each individual partial wave. Thus the magnitude of the incoming and outgoing flux must be the same. The the flux due to the incoming wave has remain unchanged. Therefore, it must be that the outgoing flux has also remain unchanged. This in turn implies the following set of relations

$$|1 + f_m e^{i\pi/4}\sqrt{2\pi k}| = 1 \tag{3.51}$$

$$\Rightarrow 1 + f_m e^{i\pi/4}\sqrt{2\pi k} = e^{2i\delta_m} \tag{3.52}$$

$$\Rightarrow f_m = \frac{e^{2i\delta_m} - 1}{\sqrt{2\pi k}} e^{-i\pi/4} \tag{3.53}$$

In equation (3.52), we have derived in two dimensions a phase shift defined by δ_m on the outgoing wave. The factor of 2 is a convention defined for mathematical convenience as will be seen in the next section. For later reference, the wavefunction may now be written as

$$\psi = \phi + \left(\frac{e^{2i\delta_0} - 1}{2} \right) 4iG(r, r'; E) \tag{3.54}$$

3.7 Calculation of Phase Shifts

Here we detail, in a manner entirely analogous to the three-dimensional problem found in various texts, determination of the scattering phase shift in terms of the value of the logarithmic derivative radius $r = R$ outside the range of the scatterer.

Within the region $r < R$ containing the scatterer and the origin, the interior wavefunction must be only be a sum of basis functions with radial part $J_l(kr)$, Bessel functions of the first kind. As we saw in the previous section, for $R > r$, we are able to include basis functions with radial part $Y_l(kr)$. By continuity of the wavefunction and its derivative, the logarithmic derivatives of the interior and exterior wavefunctions must match. Numerical determination of the logarithmic derivative of the interior wavefunction approaching $r = R$ will allow for calculation of the phase shift seen in the exterior wavefunction.

We start off by rewriting the radial part of of the asymptotic form of the wavefunction (3.50) as

$$A_l(r) \equiv \left(\frac{e^{2i\delta_l}}{2} H_l^{(1)}(kr) + \frac{1}{2} H_l^{(2)}(kr) \right) = e^{i\delta_l} \{\cos\delta_l J_l(kr) - \sin\delta_l Y_l(kr)\} \tag{3.55}$$

We now take the logarithmic derivative of the radial function and evaluate it at $r = R$. Some texts use the convention $\beta_l \equiv r\frac{d}{dr}\ln A_l(r)$ to determine the phase shift. Because we will use this result later, we adopt the convention $B_l \equiv \frac{d}{dr}\ln A_l(r)$. The logarithmic derivative of the radial wavefunction evaluated at $r = R$ is then

$$B_l = \frac{1}{A_l}\frac{dA_l}{dr}|_{r=R} \tag{3.56}$$

$$= \frac{J_l'(kR)\cos\delta_l - Y_l'(kR)\sin\delta_l}{J_l(kR)\cos\delta_l - Y_l(kR)\sin\delta_l} \tag{3.57}$$

Rewriting to solve for $\tan\delta_l$, we get

$$\tan\delta_l = \frac{J_l'(kR) - B_l J_l(kR)}{Y_l'(kR) - B_l Y_l(kR)} \tag{3.58}$$

Thus determining the phase shift is reduced to the problem of solving for the logarithmic derivative B_l at $r = R$.

3.8 The Optical Theorem

In this section, we derive a relation between the scattering amplitude in the forward direction and the total cross-section known as the optical theorem.

Using equation (3.53), we can derive a more explicit expression for the total cross-section in terms of the phase shifts imparted on each of the scattered waves. First, we rewrite (3.53) as

$$f_m = \sqrt{\frac{2}{\pi k}} e^{i\delta_m} \sin\delta_m e^{i\pi/4} \tag{3.59}$$

and calculate the cross-section as follows:

$$\sigma = \int \frac{d\sigma}{d\theta} d\theta = \int |f(\theta)|^2 d\theta \tag{3.60}$$

$$= \int \sum_{m',m} \frac{2}{\pi k} e^{i(\delta_m' - \delta_m)} \sin\delta_{m'} \sin\delta_m e^{(m-m')\theta} d\theta \tag{3.61}$$

$$= \frac{2}{\pi k} 2\pi \sum_m \sin^2\delta_m \tag{3.62}$$

$$\sigma = \frac{4}{k}\sum_m \sin^2\delta_m \tag{3.63}$$

The relevant quantity to which we will compare the cross-section is the imaginary part of the forward scattering amplitude. The calculation is again straightforward:

$$\text{Im }\{e^{-i\pi/4} f(\theta = 0)\} = \text{Im }\{e^{-i\pi/4} \sum f_m e^{im\theta}|_{\theta=0}\} = \sqrt{\frac{2}{\pi k}} \sum \sin^2\delta_m \tag{3.64}$$

Comparison of these two quantities yields the optical theorem in two dimensions:

$$\sigma = \sqrt{\frac{8\pi}{k}} \text{Im }\{e^{-i\pi/4} f(\theta = 0)\} \tag{3.65}$$

3.9 The S matrix

In section 3.4, we demonstrated for a finite range potential far from the scatterer that the wavefunction asymptotically propagates outward freely, approaching some set form, say ϕ_{asympt}. At the same time, we began our discussion of scattering by assuming that some initial wave ϕ_{inc} came in to scatter off of our potential. As discussed in numerous texts ([22], [14], [25] among others), this motivates the definition of the scattering operator S defined by the relation

$$\phi_{\text{asympt}} = S\phi_{\text{inc}} \tag{3.66}$$

with the S-matrix being the matrix elements $\langle\chi_\alpha|S|\chi_\beta\rangle$ of the S operator for some set of basis functions χ_α. Furthermore, because total flux of the system must be conserved, we know that

$$\begin{aligned} \langle\phi_{\text{inc}}|\phi_{\text{inc}}\rangle &= \langle\phi_{\text{asympt}}|\phi_{\text{asympt}}\rangle & (3.67) \\ &= \langle\phi_{\text{inc}}|S^\dagger S|\phi_{\text{inc}}\rangle & (3.68) \\ \Rightarrow S^\dagger S &= \hat{1} & (3.69) \end{aligned}$$

Under the assumption that flux is conserved, we have that S must be a unitary operator and that the S-matrix is unitary. Looking back at our partial wave analysis in section 3.6, we see that we chose a convenient basis in which the S-matrix was diagonal - our incoming states $|E, m, \text{in}\rangle$ were unaffected while our outgoing states $|E, m, \text{out}\rangle$, because of flux conservation or equivalently, unitarity of the S-matrix, underwent a phase shift. A consequence of comparison between the cross-section and imaginary part of the forward scattering amplitude, both written in terms of the phase shift, allowed us to deduce the optical theorem. As discussed in [14] and [25], the optical theorem for this reason is, conversely, interpreted as a statement of unitarity of the S-matrix. In particular, calculation of the diagonal element of the S-matrix would also have lead to the optical theorem [14].

Chapter 4

Low Energy Scattering

This chapter discusses scattering in the low energy limit and introduces various aspects of the s-wave scattering formalism subsequently to be used in exploring scattering in waveguides. The s-wave point scatterer model is introduced as well as multiple scattering theory and its application to s-wave scattering. Finally, renormalized t-matrix theory, of key importance in moving from free space to a confining geometry, is discussed.

4.1 Scattering in the Low Energy Limit

At low energies in three dimensions, only s-waves ($l = 0$) contribute significantly to scattering. We will demonstrate that the same phenomenon holds true in two dimensions.

First, we examine the radial wavefunction at low energies. The radial Schrodinger Equation (2.16) restated is

$$\left[\{-\frac{\hbar^2}{2\mu}(\frac{\partial^2}{\partial r^2} + \frac{1}{r}\frac{\partial}{\partial r} - \frac{m^2}{r^2})\} + V(r)\right] R(r) = ER(r) \tag{4.1}$$

Under the substitution $U(r) = \frac{2\mu V(r)}{\hbar^2}$ and $k^2 = \frac{2\mu E}{\hbar^2}$, this becomes

$$\left(\frac{m^2}{r^2} + U(r) - k^2\right) R(r) = \left(\frac{\partial^2}{\partial r^2} + \frac{1}{r}\frac{\partial}{\partial r}\right) R(r) \tag{4.2}$$

so that for $k^2 \ll |U(r)|$, the wavefunction, and hence the logarithmic derivative B_l (see section 3.7) is approximately independent of energy.

Now we calculate the phase shift (3.58)

$$\tan \delta_m = \frac{J'_m(kR) - B_m J_m(kR)}{Y'_m(kR) - B_m Y_m(kR)} \tag{4.3}$$

in the limit $k \to 0$ using asymptotic forms of the Bessel Functions:

$$J_m(kr) \quad \to \quad \frac{1}{m!}\left(\frac{k}{2}\right)^m r^m \tag{4.4}$$

$$Y_m(kr) \quad \to \quad \begin{cases} \frac{2}{\pi}\{\ln(\frac{1}{2}kr) + \gamma\} & l = 0, \\ -\frac{(m-1)!}{\pi}\left(\frac{2}{k}\right)^m \left(\frac{1}{r}\right)^m & l > 0. \end{cases} \tag{4.5}$$

For $m = 0$,

$$\tan \delta_m \to \frac{-B_m}{\frac{2}{\pi}(\frac{1}{R} - B_m \ln kR - \ln 2 + \gamma)} \sim \frac{1}{\ln k} \tag{4.6}$$

For $m > 0$,

$$\tan \delta_m = \left[-\frac{\pi R^{2m}}{m!(m-1)!2^{2m}} \cdot \frac{m - B_m R}{m + B_m R} \right] k^{2m} \sim k^{2m} \tag{4.7}$$

Because at low energy B_m is approximately constant, we see that

$$\lim_{k \to 0} \frac{k^{2m}}{\ln k} \to 0, \ \mathrm{m} > 0$$

we have that at sufficiently low energies, s-wave ($m = 0$) scattering dominates.

4.2 The S-wave Point Scatterer Model

Up to now, we have discussed scattering in the presence of general potentials. We now introduce a model for low energy scattering through what are known as "zero range potentials" or "point interactions," scatterers that only interact with the incoming wavefunction at a single point.

Because of their simplicity as a model for scattering, point interactions have received much attention in the literature [2, 7] and have found application in various settings, including scattering from arbitrary boundaries [19], chaotic systems [11], atom-atom scattering [20], and statistical mechanics [21].

We consider a specific class of these potentials, s-wave point scatterers. Under this model, the T operator from section 3.3 for a scatterer centered around the point r_i is approximated as $T(E) = |r_i\rangle s(E) \langle r_i|$ where $s(E)$ is a complex constant. Under this model, we have that the scattered wavefunction interacting with a scatterer at $\vec{r} = 0$ becomes

$$\begin{aligned} \langle r|\psi\rangle &= \langle r|\phi\rangle + \langle r|\frac{2\mu}{\hbar^2} GT|\phi\rangle & (4.8) \\ &= \phi(r) + \frac{2\mu}{\hbar^2} G(\vec{r}, 0; E) s(E) \phi(0) & (4.9) \end{aligned}$$

Assuming that the wavelength of interest is much larger than the scatterer being modeled or that we are in the low energy limit, it can be shown that this is a valid approximation [20]. Because $J_l(0) = 0$ for $l > 0$, we see the form of T is such that in free space, only the s-wave can possibly scatter. As we will see, the simplicity of this model greatly reduces the calculation of multiple scattering events.

Let us now calculate the scattering cross-section that results from using an s-wave scattering point interaction by using the method of partial waves. The scattered wave is $s\frac{2\mu}{\hbar^2}G\phi(0)$ where s is just a complex constant. Since there is no angular dependence, this point interaction clearly only scatters s-waves. The asymptotic form of the scattered wave is then

$$s\frac{2\mu}{\hbar^2} G(r, 0; E)\phi(0) \to s\frac{2\mu}{\hbar^2}\{-\frac{1}{2}\sqrt{\frac{1}{2\pi kr}} e^{i\pi/4} \frac{e^{ikr}}{\sqrt{r}}\}\phi(0) = -is\phi(0)\frac{\mu}{\hbar^2}\sqrt{\frac{1}{2\pi kr}} e^{i(kr - \pi/4)} \tag{4.10}$$

Analogous to the reasoning with equation (3.49), we derive a phase shift on the s-wave caused by the point scatterer,

$$\begin{aligned} 1 - is\phi(0)\frac{\mu}{\hbar^2} &= e^{2i\delta_0} & (4.11) \\ \Rightarrow -s\phi(0)\frac{\mu}{2\hbar^2} &= e^{i\delta_0} \sin \delta_0 & (4.12) \\ \Rightarrow \sigma = \frac{4}{k} \sin^2 \delta_0 &= \frac{\mu^2}{\hbar^4} \frac{1}{k} |s\phi(0)|^2 & (4.13) \end{aligned}$$

where in the last step, we used the fact that only the s-wave experiences a phase shift.

4.3 Constraints on the Value of S

Analogous to a general potential, the choice of $s(E)$ creates a cross-section and must satisfy the optical theorem to conserve flux. It must still hold true asymptotically that, an initial incoming wave $\phi(\vec{x})$ scattered by any finite range potential may be written in the form of equation (3.31),

$$\psi(\vec{r}) = \phi(\vec{r}) + \frac{e^{i|k|r}}{\sqrt{r}} f(\theta) \tag{4.14}$$

At the same time, for a point scatterer at the origin with the incident plane wave $\phi(r)$, we get that

$$\psi(\vec{r}) = \phi(\vec{r}) + s\frac{2\mu}{\hbar^2} G(r, 0; E)\phi(0) \tag{4.15}$$

thus we see that $\frac{e^{i|k|r}}{\sqrt{r}} f(\theta, k) = sG(r, r'; E)\phi(0)$ which is independent of θ; this is expected since only the rotationally symmetric s-wave scatters. Relating this to the scattering amplitude, we have for $f(\theta)$ by comparing (4.14) and (4.15) for the scattering amplitude,

$$\begin{aligned} f(\theta) &= -\frac{im}{2\hbar^2}\sqrt{\frac{2}{\pi k}} e^{-i\pi/4} s\phi(0) & (4.16) \\ &= -\frac{\mu}{2\hbar^2}\sqrt{\frac{2}{\pi k}} e^{i\pi/4} s\phi(0) & (4.17) \end{aligned}$$

As was done earlier using partial wave analysis, using the relation $\frac{d\sigma}{d\theta} = |f(\theta)|^2$, one can re-derive the cross-section (4.13) of a point scatterer s. We have derived the scattering amplitude in order to use it with the optical theorem (3.65) from section 3.8 which, to restate, asserts

$$\sigma = \sqrt{\frac{8\pi}{k}} \mathrm{Im}(f(\theta = 0)e^{-i\pi/4}) \tag{4.18}$$

If we apply this to equations (4.17) and (4.13), we get the relation

$$(\frac{m}{2\hbar^2})|s\phi(0)|^2 = -\mathrm{Im}\ (s\phi(0)) \tag{4.19}$$

which simplifies to

$$(\frac{m}{2\hbar^2})|s|^2 = -\mathrm{Im}\ s \tag{4.20}$$

For an s-wave scatterer, satisfaction of this equation is equivalent to satisfaction of the optical theorem.

4.4 Choosing s(E)

There are numerous methods of choosing $s(E)$. Provided that the constraint of equation (4.20) is satisfied, the choice of $s(E)$ may be made freely and according to the phenomenon being modeled.

Perhaps the most straightforward way, if modeling is done at a single energy, is to define $s(E)$ in terms of the phase shift using equation (4.11). This has been effective used in modeling quantum corrals [11] and proposed as a means of studying scattering off of a step edge [5].

In proximity resonance as seen in [12, 13] on the other hand requires $s(E)$ to be defined on a range of energies with a resonance peak in cross section. One possibility for this, creating a resonance width $2\sqrt{k}\gamma^2$ in two-dimensional scattering is [13]

$$s(k) = \frac{\sqrt{\frac{2}{\pi}} e^{i\pi/4}\gamma^2}{E_0 - k^2/2 - i\sqrt{k}\gamma^2} \tag{4.21}$$

For simplicity, $s(E)$ may be chosen to simulate a hard disk potential. In this case, analogous to hard sphere scattering as treated in [22], we require for a disk of radius a that the s-wave go to zero. In two dimensions, this leads to

$$J_0(ka) + \frac{2\mu}{\hbar^2} G(a,0;E) s J_0(0) = 0 \tag{4.22}$$

$$\Rightarrow s(E) = -\frac{\hbar^2}{2\mu} \frac{J_0(ka)}{G(a,0;E)} \tag{4.23}$$

$$s(E) = \frac{-i2\hbar^2}{\mu} \frac{J_0(ka)}{H_0^{(1)}(ka)} \tag{4.24}$$

applying asymptotic forms for J_0 and $H_0^{(1)}$, this becomes

$$s(E) = \left(\frac{\hbar^2}{\mu}\right) \frac{2}{i + \frac{2}{\pi}\left[\ln(\frac{1}{2}ka) + \gamma\right]} \tag{4.25}$$

4.5 Multiple Scattering and the S-wave Point Scatterers

So far, the scattering that has been considered takes place within what we might consider a "single" scattering region. The scatterer potential was considered to have some finite range and the asymptotic limit was taken as the point of observation. In many experiments however, it is behavior of the wave in a non-asymptotic region or the interactions among scatterers that is of interest as in the modeling of electron scattering off of Fe adatoms on a Cu(111) surface in quantum corrals or quantum proximity resonances [11, 12]. In the case of quantum corrals, electron waves scatter off of multiple adatoms before exiting the system while in proximity resonances, interactions between s-wave scatterers cause the development of more resonances. To account for these scattering events, there is multiple scattering theory.

For multiple scattering theory, we assume a potential V that is the sum different scattering regions $V = \sum V_i$. Then the scattered wavefunction may be written as

$$\psi = \phi + GV\psi = \phi + GT\phi \tag{4.26}$$

Because a good deal of operator manipulation will occur we have, for convenience, swallowed up the term $\frac{2\mu}{\hbar^2}$ into G, the Green's function (now $G \equiv (E - H_0 + i\epsilon)^{-1}$). From (3.16) and our assumptions about V, it is possible to rewrite $T \equiv \sum T_i$ as

$$T = V + VG_0T \tag{4.27}$$

$$\Rightarrow T_i = V_i + V_iG_0T = V_i + V_iG_0\left(\sum_j T_j\right) \tag{4.28}$$

$$\Rightarrow (1 - V_iG_0)T_i = V_i + V_iG_0\left(\sum_{j\neq i} T_j\right) \tag{4.29}$$

$$\Rightarrow T_i = (1 - V_iG_0)^{-1}V_i + (1 - V_iG_0)^{-1}V_iG_0\left(\sum_{j\neq i} T_j\right) \tag{4.30}$$

Recalling equation (3.21), we see that $(1 - V_iG_0)^{-1}V_i = t_i$, where t_i is the transfer operator we would see in equation (4.27) had our original potential only been V_i. Equation (4.30) may thus be interpreted as the scattering from the region V_i is equals the the original scattering resulting from V_i plus the scattering of flux reaching V_i as a result of the other potentials V_j. If our sum for V_i runs from 1 to N, we now have a set of N equations to solve for N operators T_i:

$$\begin{bmatrix} T_1 \\ \vdots \\ T_N \end{bmatrix} = \begin{bmatrix} t_1 \\ \vdots \\ t_N \end{bmatrix} + \begin{bmatrix} 0 & t_1 & \dots & t_1 \\ \dots & \dots & \dots & \dots \\ t_n & \dots & t_n & 0 \end{bmatrix} G_0 \begin{bmatrix} T_1 \\ \vdots \\ T_N \end{bmatrix} \tag{4.31}$$

Abbreviating this as

$$\mathbf{T} = \mathbf{t} + \mathbb{T}G\mathbf{T} \tag{4.32}$$

we can formally solve for $\mathbf{T}$ as

$$\mathbf{T} \quad = \quad (1 - \mathbb{T}G)^{-1}\mathbf{t} \tag{4.33}$$

For the s-wave point scatterer model, we have that $t_j = s_j|r_j\rangle\langle r_j|$ and $\mathbf{T}$ takes on a particularly simple form. For the equation $\psi = \phi + GT\phi$, we start by solving for $\langle r|T_i|\phi\rangle$ using equation (4.30):

$$\langle r|T_i|\phi\rangle \quad = \quad \langle r|t_i|\phi\rangle + \sum_{i\neq j}\langle r|t_i G_0 T_j|\phi\rangle \tag{4.34}$$

$$= \quad \delta(r - r_i)s_i \left(\phi(r_i) + \sum_{i\neq j}\langle r_i|G_0 T_j|\phi\rangle \right) \tag{4.35}$$

$$\tag{4.36}$$

Because (4.35) has a delta function in it, we only $\langle r_i|T_i|\phi\rangle$ is non-zero. This allows us to further simplify (4.35) as

$$\langle r_i|T_i|\phi\rangle \quad = \quad \delta(0)s_i \left(\phi(r_i) + \sum_{i\neq j} G(r_i, r_j; E)\langle r_j|T_j|\phi\rangle \right) \tag{4.37}$$

Now if we define

$$\alpha_i \equiv \frac{\langle r_i|T_i|\phi\rangle}{\delta(0)s_i} \tag{4.38}$$

we have from (4.37) that

$$\alpha_i = \phi(r_i) + \sum_{i\neq j} G(r_i, r_j; E)s_j\alpha_j \tag{4.39}$$

This yields a matrix equation through which we can solve for α_i

$$\vec{\alpha} = \vec{\Phi} + \begin{bmatrix} 0 & G(r_1, r_2) & \dots & \dots & G(r_1, r_N) \\ G(r_2, r_1) & 0 & G(r_2, r_3) & \dots & G(r_2, r_N) \\ \dots & \dots & \dots & \dots & \dots \\ G(r_N, r_1) & \dots & \dots & G(r_N, r_{N-1}) & 0 \end{bmatrix} \vec{\alpha} \tag{4.40}$$

$$\Rightarrow \vec{\alpha} = \left(I - [G]\right)^{-1} \vec{\Phi} \tag{4.41}$$

Substituting back into equation (4.26), we have that

$$\psi(r) \quad = \quad \phi(r) + \langle r|GT|\phi\rangle \tag{4.42}$$

$$= \quad \phi(r) + \sum_i G(r, r_i)\langle r_i| \sum_i T_i|\phi\rangle \tag{4.43}$$

$$= \quad \phi(r) + \sum_i G(r, r_i)s_i\alpha_i \tag{4.44}$$

Thus in the s-wave point scatterer model, solving for the scattered wavefunction in the presence of multiple potentials is essentially simplified to the task of inverting a single matrix.

4.6 Scattering in the Presence of Background Potentials

For this section, we use the convention that $G_0 \equiv (E - H_0 + i\epsilon)^{-1}$. The s-wave point scatterer model makes use of the transfer operator, defined by equation (3.21) in section 3.3. From the definition of the transfer operator (restated here),

$$T = V(1 - G_0 V)^{-1} \tag{4.45}$$

it is clear that T is dependent on the potential V of the system. We expect this from multiple scattering - a new potential added to the system contributes extra scattering interactions. For the case of point scatterers, finding "effective" s-values α_i turned out to be a straightforward calculation. In the next chapter however, we will want to consider scattering in waveguides, contributing a background potential V, in the presence of s-waves scatterers whose strengths in free space are known. For this, we turn to renormalized t-matrix theory as developed by A. Lupu-Sax [18].

Renormalized t-matrix theory relates the T operator of a given "background" potential V_0 with Green's function G_0 to the T operator of a potential $V = V_0 + V'$ with Green's function G_V. For brevity, we state here the result; formal derivations may be found in [18] and [20].

$$\begin{aligned} T_V(E) &= \{1 - T_0(E)(G_V(E) - G_0(E))\}^{(-1)} T_0(E) & (4.46) \\ &= \left(\frac{1}{1 - T_0(E)(G_V(E) - G_0(E))} \right) T_0(E) & (4.47) \end{aligned}$$

For an s-wave point scatterer in free space with $t_0(E) = |r\rangle s(E) \langle r|$, $t_V(E)$ remains a delta function and (4.47) relates the complex constants $s_V(E)$ and $s_0(E)$ according to the formula

$$\begin{aligned} s_V(E) &= \lim_{r \to r'} \frac{1}{1 - s_0(E)(G_V(r, r'; E) - G_0(r, r'; E))} s_0(E) & (4.48) \\ \Rightarrow \frac{1}{s_V(E)} &= \frac{1}{s_0(E)} - \lim_{r \to r'} (G_V(r, r'; E) - G_0(r, r'; E)) & (4.49) \end{aligned}$$

Chapter 5

Scattering in Waveguides

We now translate the results of the previous chapters, which have primarily dealt with scattering in free space, to a model two-dimensional waveguide system. While we deal with a particular model system, many of the results derived will readily translate to other two- and three-dimensional waveguide systems.

We consider an infinite wire in the x-direction, but confined in the y-direction by infinitely hard walls a distance W apart. To consider scattering in this system, we begin by deriving the Green's function for this system as well as the renormalized scattering strength of an s-wave scatterer relative to its strength in free-space.

Having established the basic tools for studying scattering in waveguides, we proceed to derive formulas using the s-wave point scatterer model for cross-section, the optical theorem, and phase shift. Finally, we conclude with a discussion of resonant scattering, conductance dips at threshold energies in the waveguide, and the optical theorem in a waveguide for a general potential.

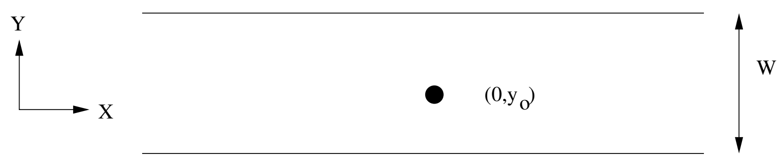

Figure 5.1: Coordinate set-up for the model system being considered

5.1 Basis Functions

The natural basis functions for this system are of the form

$$\langle x, y|E, m\rangle = X_m(y) \cdot (Ae^{ik_x^{(m)}x}) \tag{5.1}$$

where the transverse modes $X_m(y)$ are the usual particle in a box basis functions

$$X_m(y) = \sqrt{\frac{2}{W}}\sin(k_y^{(m)}y) = \sqrt{\frac{2}{W}}\sin(\frac{m\pi}{L}y) \tag{5.2}$$

with $k_y^{(m)}$ representing the transverse wavenumber and $k_x^{(m)} = \sqrt{\frac{2mE}{\hbar^2} - k_y^2}$ the longitudinal wavenumber, here proportional to momentum in the x-direction. While the wave in the y-direction has been normalized in the usual way, the normalization constant A in the x-direction may be normalized either as in Section 2.1.1 to a delta function or as in Section 2.2.2 to unit flux through the wire. Because we will be interested in flux transmission, we will work primarily with unit flux normalization so that the final expression for our a basis function is

$$\langle x, y|E, m\rangle = X_m(y)\frac{e^{ik_x^m x}}{\sqrt{k_x^m}} = \sqrt{\frac{2}{Wk_x^m}}\sin(\frac{m\pi}{W}y)e^{ik_x^m x} \tag{5.3}$$

5.2 Green's Function for a Hard Wire

While there are various methods of calculating the Green's function of a system $G(\vec{x}, \vec{x'}) = \frac{\hbar^2}{2\mu}\langle\vec{x}|\frac{1}{E-H_0+i\epsilon}|\vec{x'}\rangle$, we detail here one which uses the method of images from electrostatics, similar to that employed in [6]. The more general method of eigenfunction expansion is detailed in Appendix A.

The infinite wire will have hard walls at $y = 0$ and $y = W$. Because of translational invariance in the x-direction, we may also assume that $\vec{x'} = (0, y')$ in deriving $G(\vec{x}, \vec{x'})$. Since $V = 0$ inside the wire, the differential equation to be satisfied by the Green's function is from (3.13),

$$(\nabla^2 + k^2)G(x, x'; k) = \delta^{(2)}(x - x') \tag{5.4}$$

now subject to the boundary conditions

$$G(\vec{x}, \vec{x'})|_{y=0} = G(\vec{x}, \vec{x'})|_{y=W} = 0 \tag{5.5}$$

The two-dimensional free Green's function $G_0^+(r, r'; k) = -\frac{-i}{4}H_0^{(1)}(k|r - r'|)$ satisfies (5.4), so if we can add solutions satisfying the homogeneous equation

$$(\nabla^2 + k^2)F = 0 \tag{5.6}$$

then we will have the Green's function to the wire. As suggested above, we will do this by adding a series of images of the two-dimensional free Green's function.

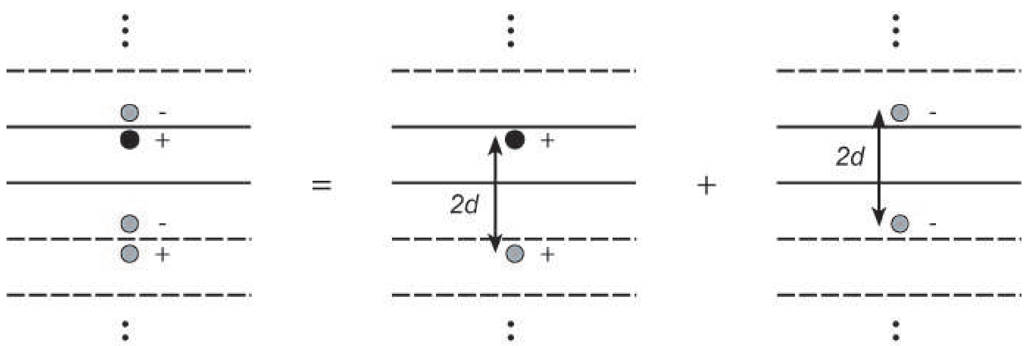

Figure 5.2: The original Green's function is reflected to form an array of itself and images with alternating sign. As illustrated, this may be broken down into two separate sums.

If we consider the sum

$$G = -\frac{i}{4}\{\sum_{n=-\infty}^{\infty} H_0^{(1)}(k|r - (0, 2Wn + y')|) - \sum_{n=-\infty}^{\infty} H_0^{(1)}(k|r - (0, 2Wn - y')|)\} \tag{5.7}$$

as illustrated in Figure 5.2, we find that it satisfies the boundary conditions in (5.5) as G is anti-symmetric with respect to reflection around $y = Wn$. Furthermore, we have for $y \in [0, W]$ that

$$(\nabla^2 + k^2)G = \sum_{n=-\infty}^{\infty} \delta(x)\delta(y - (2Wn + y')) - \sum_{n=-\infty}^{\infty} \delta(x)\delta(y - (2Wn - y')) \tag{5.8}$$

$$= \delta(x)\delta(y - y'), \text{ for } y \in [0, W] \tag{5.9}$$

Therefore $G(x, y; E)$ in equation (5.7) must be the Green's function of the wire. In principle, this turns any scattering problem in the hard wire system we have defined into one in free space, and in fact, we will show in the next section that it is possible to calculate renormalized scattering strengths in this manner.

In practice however, calculating the Green's function requires that one must truncate the sum, and for $x \gg (y' + 2Wn_{max})$, it converges quite slowly. This is because asymptotically $H(kr) \sim \frac{e^{ikr}}{\sqrt{r}} \sim \frac{e^{ikr}}{\sqrt{x}}$ so that to begin converging when calculating G(x,y,x',y';E), we need that $(y' + 2Wn_{max})$ on the order of x as seen in Figure 5.3.

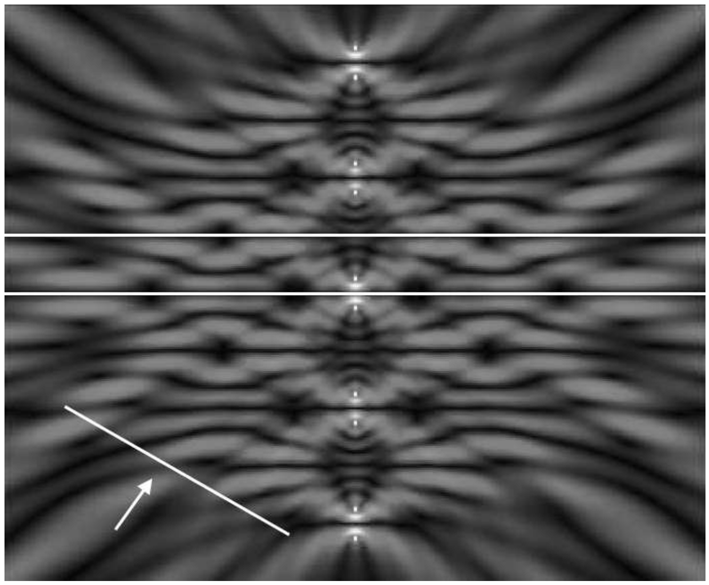

Figure 5.3: A plot of the absolute value of the free space Green's function and nine of its images. Lines have been added to demarcate the location of the real wire as from its images. The line marked by the arrow is a visual aid demonstrating a rough convergence limit caused by truncating the Green's function sum. To calculate $G(x, y, 0, y'; E)$, we see that we must have the maximum y extent of the array on the order of x. Relative intensity in the plot goes from black (low density) to white (high density). The grayscale has been omitted due to the qualitative nature of the plot.

To avoid this problem, it is more convenient to express the Green's function in its eigenfunction expansion which we state below; a derivation of this may be found in Appendix A.

$$G(\vec{x}, \vec{x'}) = \frac{-i}{2} \sum_{m=1}^{\infty} \chi_m(y)\chi_m(y') \frac{e^{ik_x^{(m)}|x-x'|}}{k_x^{(m)}} \tag{5.10}$$

In [17], it is demonstrated how an infinite sum of Hankel functions is able to produce a sum of plane waves. Physically, one might expect the periodic array of images we have created to act as a diffraction grating on incoming plane waves so this should not be too surprising.

The evanescent modes decay exponentially so that for large x, the Green's function converges quickly. However, the original sum (5.7) contained a Hankel function centered at $(0, y')$, so we know there must be logarithmic singularity hidden in the sum of the evanescent modes. Using Kummer's Method of accelerated convergence [1], we make this explicit rewriting the sum as

$$\begin{aligned} G_V(\vec{r}, \vec{r}_0; k) = -\frac{i}{2} \sum_{m=1}^{\infty} \chi_m(y)\chi_m(y_0)\left(\frac{1}{k_x^{(m)}} e^{ik_x^{(m)}|x-x_0|} + \frac{iW}{m\pi} e^{-\frac{m\pi}{W}|x-x_0|}\right) \\ - \frac{1}{4\pi} \ln \frac{\cos\left[\frac{\pi}{W}(y-y_0)\right] - \cosh\left[\frac{\pi}{W}(x-x_0)\right]}{\cos\left[-\frac{\pi}{W}(y+y_0)\right] - \cosh\left[\frac{\pi}{W}(x--x_0)\right]} \end{aligned} \tag{5.11}$$

the details of this calculation can be found in Appendix B. In [18] it is demonstrated that rewriting the sum in this manner makes the sum converge uniformly.

5.3 Renormalized Scattering Strength

It was noted in section 4.4 that for an s-wave scatterer, as long $s(E)$ is chosen such that flux is conserved, there is freedom in choosing it. However, because the effect of a scatterer in a waveguide ultimately includes any order of scattering between itself and the confining potential, its strength $s(E)$ defined in an arbitrary manner satisfying the optical theorem buries the notion of the scatterer's intrinsic strength. For this reason, it is of use to define a scatterer's strength in the waveguide according to its freespace strength.

As discussed in section 4.6, when a of background potential is added to a system, the effective strength of a scatterer also changes. This may be interpreted as a multiple scattering effect between the the scatterer and the newly added background potential. Relative to its original scattering strength, the new strength of a zero-range scatterer, expressed in terms of its t-matrix, is

$$\tilde{s} = \lim_{r\to r'} \frac{s}{1 - s(\frac{2\mu}{\hbar^2})(G_V(r,r';E) - G_0(r,r';E))} \quad (5.12)$$

$$\Rightarrow 1/\tilde{s} = 1/s - \lim_{r\to r'} \frac{2\mu}{\hbar^2}(G_V(r,r';E) - G_0(r,r';E)) \quad (5.13)$$

Depending on the convergence acceleration method used, the form of $\tilde{s}$ may appear slightly different according to the function used to extract the singularity. Here we present one form of the renormalized scattering strength as derived in [18]. $\frac{2\mu}{\hbar^2}(G_V(r,r';E) - G_0(r,r';E))$ takes the limit

$$\lim_{r\to r'} \frac{2\mu}{\hbar^2}(G_B^+(r,r',E) - G_0^+(r,r',E)) = - \frac{2i\mu}{W\hbar^2}\sum_{n=1}^{N}\sin^2(\frac{\pi n y}{W})[\frac{1}{k_x^n} - \frac{W}{\pi i n}] - \frac{2\mu}{W\hbar^2}\sum_{n>N}^{\infty}\sin^2(\frac{\pi n y}{W})[\frac{1}{\kappa_n^x} - \frac{W}{\pi n}] - \frac{\mu}{2\pi\hbar^2}\ln[\sin^2\frac{\pi y}{W}] + \frac{\mu}{\pi\hbar^2}\ln[\frac{\pi}{2W}] + \frac{\mu}{\pi\hbar^2}\ln[|r-r'|] + \{\frac{i\mu}{2\hbar^2} - \frac{\mu}{2\hbar^2}Y_0^{(R)}(0) - \frac{\mu}{\pi\hbar^2}\ln k - \frac{\mu}{\pi\hbar^2}\ln|r-r'|\}$$

where $k^2 = k_x^2 + k_y^2$, $k_x^n = \sqrt{\frac{2\mu E}{\hbar^2} - (\frac{n\pi}{W})^2}$ is the wavenumber in the x-direction, and $\kappa_x^n = \sqrt{(\frac{n\pi}{W})^2 - \frac{2\mu E}{\hbar^2}}$. This simplifies to

$$\lim_{r\to r'} \frac{2\mu}{\hbar^2}(G_B^+(r,r',E) - G_0^+(r,r',E)) = -\frac{2i\mu}{W\hbar^2}\sum_{n=1}^{N}\sin^2(\frac{\pi n y}{W})[\frac{1}{k_x^n} - \frac{W}{\pi i n}] - \frac{2\mu}{W\hbar^2}\sum_{n>N}^{\infty}\sin^2(\frac{\pi n y}{W})[\frac{1}{\kappa_n^x} - \frac{W}{\pi n}] - \frac{\mu}{2\pi\hbar^2}\ln[\sin^2\frac{\pi y}{W}] + \frac{\mu}{\pi\hbar^2}\ln[\frac{\pi}{2Wk}] + \frac{i\mu}{2\hbar^2} - \frac{\mu}{2\hbar^2}Y_0^{(R)}(0) \quad (5.14)$$

Now using equation (5.13), we have for the renormalized scattering strength

$$1/\tilde{s}(E) = 1/s(E) + \lim_{r\to r'} \frac{2\mu}{\hbar^2}(G_B^+(r,r',E) - G_0^+(r,r',E)) = \frac{1}{s(E)} + \frac{2i\mu}{W\hbar^2}\sum_{n=1}^{N}\sin^2(\frac{\pi n y}{W})[\frac{1}{k_x^n} - \frac{W}{\pi i n}] + \frac{2\mu}{W\hbar^2}\sum_{n>N}^{\infty}\sin^2(\frac{\pi n y}{W})[\frac{1}{\kappa_x^n} - \frac{W}{\pi n}] + \frac{\mu}{2\pi\hbar^2}\ln[\sin^2\frac{\pi y}{W}] - \frac{\mu}{\pi\hbar^2}\ln[\frac{\pi}{2Wk}] - \frac{i\mu}{2\hbar^2} + \frac{\mu}{2\hbar^2}Y_0^{(R)}(0) \quad (5.15)$$

where $Y_0^{(R)}(0) \equiv \frac{2(\gamma - \ln 2)}{\pi}$ is the regular part of the Neumann function. An alternate form of (5.15) may be found in Appendix B.

It is interesting to see that because the hard wire scattering can be mapped to one in free space, we can also derive the renormalized scattering strength both for a single and multiple s-wave scatterers. Here we do the calculation for a single scatterer in a wire. The multiple scattering case is detailed in Appendix C. The final solution will be of the form

$$\psi(r) = \phi(r) + s \sum_k \frac{2\mu}{\hbar^2} G_0(r, r_k) \cdot \alpha_k \tag{5.16}$$

where r_k represents the position of the scatterer in the kth position with the actual scatterer at position r_0, s the scatterer strength - here a constant for the scatterer and its images, and α_k the amplitude that reaches the scatterer at r_k. By anti-symmetry (via reflection across the line $y = nW$), it must be that $\alpha_k = (-1)^k \alpha_0$ and by the usual multiple scattering argument that

$$\alpha_0 = \phi(r_0) + s \sum_{k \neq 0, k=-\infty}^{\infty} \frac{2\mu}{\hbar^2} G_0(r_0, r_k) \alpha_k \tag{5.17}$$

combining the two together, we have that

$$\alpha_0 = \phi(r_0) + s\lambda\alpha_0 \tag{5.18}$$

$$\Rightarrow \alpha_0 = \frac{\phi(r_0)}{1 - s\lambda} \tag{5.19}$$

where

$$\lambda = \frac{2\mu}{\hbar^2} \sum_{k \neq 0, k=-\infty}^{\infty} (-1)^k G_0(r_0, r_k) \tag{5.20}$$

Our final wavefunction is then

$$\psi(r) = \phi(r) + \frac{s}{1 - s\lambda} \{ \sum_{k=-\infty}^{\infty} \frac{2\mu}{\hbar^2} G_0(r, r_k) (-1)^j \} \phi(r_0) \tag{5.21}$$

Thus from equation (5.21), we have derived both the Green's function for the wire (in brackets) and the renormalized scattering strength $\tilde{s} = \frac{s}{1-s\lambda}$. That we knew to renormalize with the factor $\lambda = G_V(r, r'; E) - G_0(r, r'; E)$ came naturally from our multiple scattering treatment of the problem.

5.4 Cross-Section (or Not) in a Waveguide

Now that we have derived an expression for the renormalized scattering strength and the Green's function of the wire, we may derive an expression for the cross-section of an s-wave scatterer. As in section 3.5, we will want to define something analogous to equation (3.35), the differential cross-section. For the case of the wire, it does not make sense to consider the differential cross-section in terms of the angle of scattering relative to the direction of the incoming wave. The incoming wave has no definite k-value in the y-direction and the angle over which to integrate asymptotically goes to 0. Instead, we calculate the flux with respect to dy.

Placing our scatterer at $(0, y')$ and sending in a basis function, recall we have that

$$\begin{aligned}
\langle x|E,m\rangle &= \psi_m^{\text{inc}} = \chi_m(y)\frac{e^{ik_x^{(m)}x}}{\sqrt{k_x^{(m)}}} && (5.22)\\
\Rightarrow \psi_{\text{scat}} &= \tilde{s}\frac{2\mu}{\hbar^2}G(r,r';E)\psi_m^{\text{inc}}(r') && (5.23)\\
&= \frac{-i\mu\tilde{s}}{\hbar^2}\{\sum_{n=1}^{\infty}\chi_n(y)\chi_n(y')\frac{e^{ik_x^{(n)}|x-x'|}}{k_x^{(n)}}\}\frac{\chi_m(y')}{\sqrt{k_x^{(m)}}} && (5.24)
\end{aligned}$$

Now calculating the flux density for the incoming and scattered components we have

$$\begin{aligned}
j_y^{\text{inc}} &= \text{Im }\{\psi_{\text{inc}}^*\frac{\partial}{\partial x}\psi_{\text{inc}}\} && (5.25)\\
&= \chi_m(y)^2 && (5.26)
\end{aligned}$$

and for $x > 0$,

$$\begin{aligned}
j_y^{\text{scat}} &= \text{Im }\{\psi_{\text{scat}}^*\frac{\partial}{\partial x}\psi_{\text{scat}}\} && (5.27)\\
&= \frac{\chi_m(y')^2}{k_x^{(m)}}(\frac{\mu}{\hbar^2})^2\tilde{s}^2\sum_m\sum_p\chi_m(y)\chi_p(y)\chi_m(y')\chi_p(y')\frac{e^{i(k_x^{(m)}-k_x^{(p)})(x-x')}}{k_x^{(p)}} && (5.28)
\end{aligned}$$

The scattered flux for $x < 0$ is the same equation, but with $e^{-i(k_x^{(m)}-k_x^{(p)})(x-x')}$. In principle, we could take $\frac{d\sigma}{dy} = \frac{|j_{\text{scat}}|}{|j_{\text{inc}}|}$ to obtain the differential cross-section and integrate this over y at $x \gg 0$ and $x \ll 0$ to obtain the total cross-section. However, the resulting form of the differential cross-section is unwieldy for this purpose - as opposed to free space, taking into account the incoming flux is no longer a matter of dividing the overall answer by a constant. Instead, we take the quotient of the total scattered flux over the total incoming flux. This yields a dimensionless quantity that we will call the *relative cross-section*.

As the incoming flux has been normalized to 1, we only have to integrate equation (5.28). This in turn is simplified by orthogonality of the transverse modes, $\int dy\chi_m(y)\chi_p(y) = \delta_{mp}$. The case for $x < 0$ yields the same result, so we multiply by 2. Thus we have as the final answer that

$$\sigma = 2\cdot\frac{\chi_m(y')^2}{k_x^{(m)}}(\frac{\mu}{\hbar^2})^2|\tilde{s}|^2\sum_{n=1}^{N}\frac{\chi_n(y')^2}{k_x^{(n)}} \tag{5.29}$$

5.5 S matrix of a Point Scatterer

The S matrix of a point scatterer is calculated here as a foundation for our later results. As usual, we place a point scatterer at $(0, y')$. Because of the separable basis of this system, it is natural to construct the S matrix in a similar manner to the usual one-dimensional scattering problem. We separate our basis functions into left- and right-moving in the x-direction $\{|E,m,+\rangle, |E,m,-\rangle\}$ and order them as $[|E,m,+\rangle, |E,m,-\rangle]$. The S matrix then takes on the form

$$\begin{bmatrix} T & R' \\ R & T' \end{bmatrix} \tag{5.30}$$

where T and R represent reflection and transmission, respectively. For energies in which only a single mode is allowed, this is simply a 2×2 matrix, which is what we would get if we were working in one dimension. It is understood that $S|E,m,+\rangle$ means sending in initial wave $|E,m,+\rangle$ from the left resulting in $T|E,m,+\rangle$ on the *right* of the scatterer and $R|E,m,+\rangle$ on the *left* of the scatterer. Without scattering, this matrix becomes the identity so we add to this the contribution from scattering. Rewriting equation (5.24), we have that (recall $x' = 0$)

$$\psi_{\text{scat}} = \frac{-i\mu\tilde{s}}{\hbar^2}\{\sum_{n=1}^{\infty}\chi_n(y)\chi_n(y')\frac{e^{ik_x^{(n)}|x|}}{k_x^{(n)}}\}\frac{\chi_m(y')}{\sqrt{k_x^{(m)}}} \tag{5.31}$$

$$= \{\sum_{n=1}^{\infty}(\frac{-i\mu\tilde{s}}{\hbar^2}\frac{\chi_n(y')\chi_m(y')}{\sqrt{k_x^{(n)}k_x^{(m)}}})\chi_n(y)\frac{e^{ik_x^{(n)}|x|}}{\sqrt{k_x^{(n)}}}\} \tag{5.32}$$

$$\Rightarrow \langle n|S|m\rangle = \delta_{mn} + (\frac{-i\mu\tilde{s}}{\hbar^2}\frac{\chi_n(y')\chi_m(y')}{\sqrt{k_x^{(n)}k_x^{(m)}}}) \tag{5.33}$$

note the absolute value in $e^{ik_x^{(n)}|x|}$ means both transmission and reflection are both generated by the scatterer so that adding in the contribution from the initial wavefunction (the identity), $T_{nm} = \delta_{mn} + R_{nm}$ where

$$R_{nm} = (\frac{-i\mu\tilde{s}}{\hbar^2}\frac{\chi_n(y')\chi_m(y')}{\sqrt{k_x^{(n)}k_x^{(m)}}}) \tag{5.34}$$

Finally, because we can take x arbitrarily far away from the scatterer, we can neglect the evanescent modes, where $\frac{\hbar^2 k_y^{((m)}}{2\mu} > E$ as they exponentially decay so that S is a finite matrix.

5.6 Unitarity Constraints on $\tilde{s}$

Now that we have derived the S matrix for the point scatterer in a wire, we will derive as in section 4.3 an analogous constraint for $\tilde{s}$, the renormalized scattering strength in the wire. To do this, we calculate the diagonal of $S^\dagger S$, knowing that since S is unitary, it must be 1.

Taking advantage of our work from the last section, the m-th element of the diagonal of $S^\dagger S$ is

$$\sum_{n=1}^{N_{\max}} |R_{nm}|^2 + |T_{nm}|^2 = 1 \tag{5.35}$$

where we have broken down the sum into reflection and transmission. Note our sum now runs from 1 to $N_{\max}$, the maximum allowed quantum number, as opposed to the $2N_{\max}$ left and right propagating modes. We then have that

$$\sum_{n=1}^{N_{\max}} |R_{nm}|^2 + |\delta_{nm} + R_{nm}|^2 = 1 \tag{5.36}$$

$$\Rightarrow |R_{mm}|^2 + |1 + R_{mm}|^2 + \sum_{n\neq m, n=1}^{N_{\max}} 2|R_{nm}|^2 = 1 \tag{5.37}$$

$$\Rightarrow (R_{mm} + R_{mm}^*) + \sum_{n=1}^{N_{\max}} 2|R_{nm}|^2 = 0 \tag{5.38}$$

$$\Rightarrow \text{Re } R_{mm} = -\sum_{n=1}^{N_{\max}} |R_{nm}|^2 \tag{5.39}$$

Now substituting for R_{nm} using (5.34), we get

$$\text{Im }(\tilde{s})\frac{\mu}{\hbar^2}\frac{\chi_m(y')^2}{k_x^{(m)}} = -|\tilde{s}|^2\frac{\chi_m(y')^2}{k_x^{(m)}}(\frac{\mu}{\hbar^2})^2\sum_{n=1}^{N_{\max}}\frac{\chi_n(y')^2}{k_x^{(n)}} \tag{5.40}$$

$$\Rightarrow \text{Im }\tilde{s} = -|\tilde{s}|^2(\frac{\mu}{\hbar^2})\sum_{n=1}^{N_{\max}}\frac{\chi_n(y')^2}{k_x^{(n)}} \tag{5.41}$$

where in the last step, we have removed the degenerate terms in the sum. It should also important to note that we have chosen transverse basis $\chi_m(y)$ that is real, which can be done for any potential $V(\vec{r})$. That is, $N_{\max}$ represents the quantum number of the maximum y-momentum. Thus analogous to (4.20), (5.41) the choice of $\tilde{s}$ is limited by unitarity.

Using equations (5.29) and (5.41), it is possible to derive alternate expressions for the scattering cross-section. We now have that

$$\sigma = -2\text{Im }\tilde{s}(\frac{\mu}{\hbar^2})\frac{\chi_m(y')^2}{k_x^{(m)}} \tag{5.42}$$

for relative cross-section seen by a particular incoming wave. We can also calculate the average relative cross-section using equation (5.42) to get

$$\bar{\sigma} = \frac{1}{2N_{\max}}\sum\sigma_n \tag{5.43}$$

$$= -\frac{1}{2N_{\max}}\text{Im }\tilde{s}(\frac{\mu}{\hbar^2})\left(2\sum_{n=1}^{N_{\max}}\frac{\chi_n(y')^2}{k_x^{(n)}}\right) \tag{5.44}$$

$$= -\frac{1}{N_{\max}}\text{Im }\tilde{s}\left(-\frac{\text{Im }\tilde{s}}{|\tilde{s}|^2}\right) \tag{5.45}$$

$$= \frac{1}{N_{\max}}\frac{(\text{Im }\tilde{s})^2}{|\tilde{s}|^2} \tag{5.46}$$

With equation (5.46), plotting the relative cross-section due to a single point scatterer becomes quite quick; this is done at several energies in Figure 5.4. A plot of the relative cross-section of a scatterer versus its position in the wire reveals several interesting features that are the result of multiple scattering of the scatterer with its image. Several resonant peaks are clearly visible spaced out across the wire. Near the edge of the wire, a sharp peak is also observed, the result of the scatterer forming a proximity p-wave resonance with its image [13]. The proximity resonance "competes" with the requirement that the cross-section goes to 0 at the edge of the wire resulting in a relatively sharp drop in relative cross section near the edge.

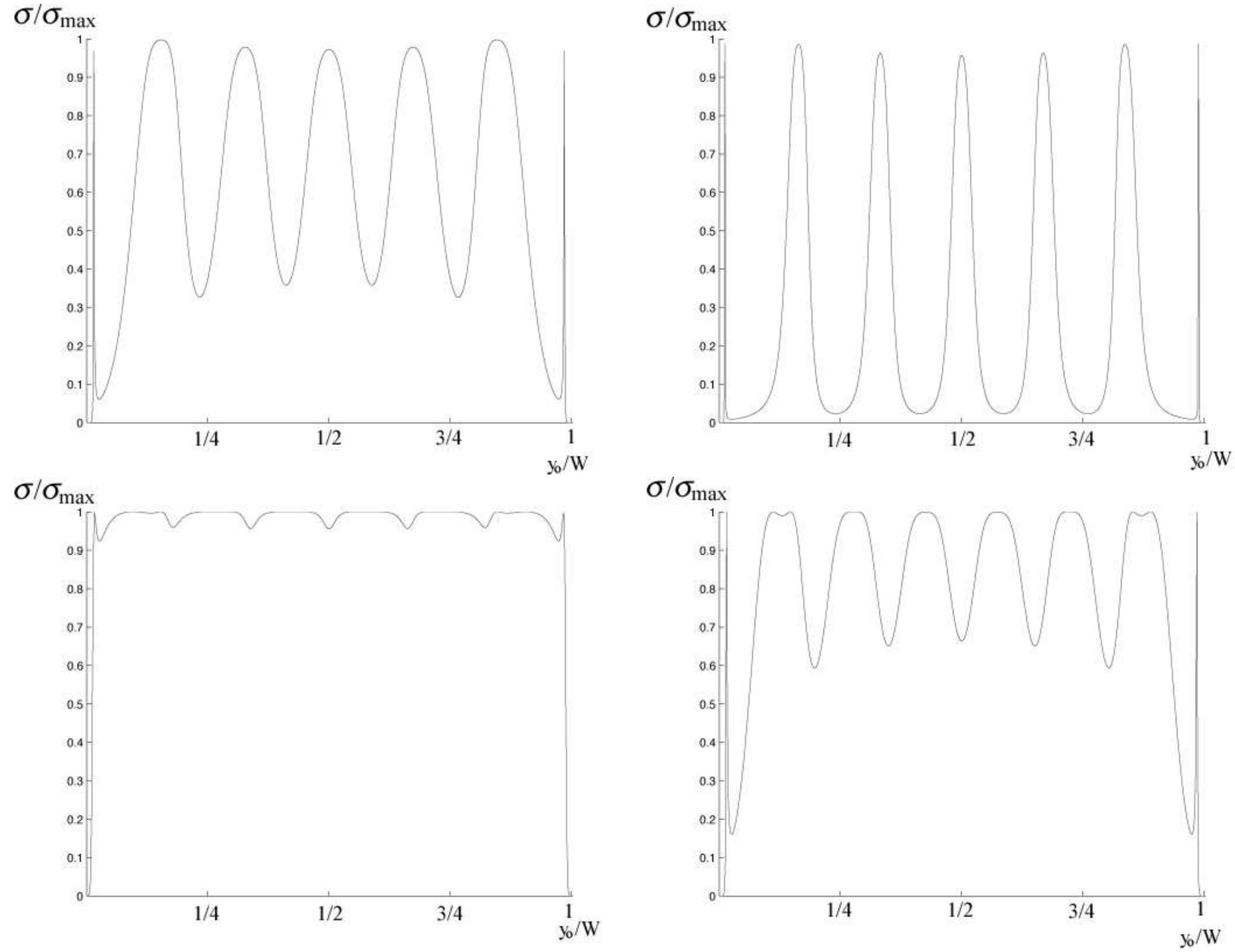

Figure 5.4: Plots of the relative cross-section versus the scatterer location y_0 in the wire at various values for kW approaching and passing through the transition from 5 to 6 allowed modes at $kW = 6\pi$ with $\hbar = \mu = 1$ and hard-sphere scattering of radius $a = 0.1$. *Top-left:* $kW = \sqrt{34}\pi$. As one might expect from the interaction of the scatterer with its images, various resonant peaks are visible within the middle of the wire. Closer to the edge when images become close to one another, narrow p-wave resonances are observed (see [12]). *Top-right:* $kW = \sqrt{35.9}\pi$, just beneath the transition energy. Cross-section peaks narrow significantly. See section 5.7 for discussion of transparency and opacity of the scatterer at the transition energy. *Bottom-left:* $kW = \sqrt{36.1}\pi$, just above the transition energy. *Bottom-right:* $kW = \sqrt{45}\pi$. Cross-section is again intermediate in appearance to the previous two limit cases.

5.7 Cross Section and Conductance Phenomena in Waveguides

Using the form (5.46) of the relative cross-section, it is possible to derive a formula for the conductance through the wire in the presence of a single scattering impurity. Using the well-known Landauer Formula for conductance [24] along with (5.41), we obtain

$$\begin{aligned} G &= \frac{2e^2}{\hbar}\text{Tr } T^\dagger T & (5.47)\\ &= \frac{2e^2}{\hbar}\left(N_{\max} - \sum_{m=1}^{N_{\max}} \text{Im } (\tilde{s})\frac{\mu}{\hbar^2}\frac{\chi_m(y')^2}{k_x^{(m)}}\right) & (5.48)\\ &= \frac{2e^2}{\hbar}\left(N_{\max} - \sum_m \sigma_m\right) & (5.49)\\ &= \frac{2e^2}{\hbar}\left(N_{\max} - \frac{(\text{Im } \tilde{s})^2}{|\tilde{s}|^2}\right) & (5.50)\end{aligned}$$

Thus a single point impurity in the wire can reduce the total conductance through the wire by at most $\frac{2e^2}{\hbar}$. In fact, as one approaches the energy threshold of a mode closing from above, this can be shown to be the limiting case, and this phenomenon has been discussed in various works [6, 9, 15]. By simple inspection of equation the renormalized scattering strength (5.15) (restated below), we provide an intuitive explanation of this phenomenon.

$$\begin{aligned} 1/\tilde{s}(E) = 1/s(E) + \lim_{r\to r'}\frac{2\mu}{\hbar^2}(G_B^+(r,r',E) - G_0^+(r,r',E)) = \\ \frac{1}{s(E)} + \frac{2i\mu}{W\hbar^2}\sum_{n=1}^{N}\sin^2(\frac{\pi n y}{W})[\frac{1}{k_x^n} - \frac{W}{\pi i n}] + \frac{2\mu}{W\hbar^2}\sum_{n>N}^{\infty}\sin^2(\frac{\pi n y}{W})[\frac{1}{\kappa_x^n} - \frac{W}{\pi n}] \\ + \frac{\mu}{2\pi\hbar^2}\ln[\sin^2\frac{\pi y}{W}] - \frac{\mu}{\pi\hbar^2}\ln[\frac{\pi}{2Wk}] - \frac{i\mu}{2\hbar^2} + \frac{\mu}{2\hbar^2}Y_0^{(R)}(0) \quad (5.51)\end{aligned}$$

The form of this equation is convenient because it separates effects of the scatterer alone, $\frac{1}{s(E)}$, from the multiple scattering contribution. As we approach a threshold energy from above, $k_x^{N_{\max}} \to 0$ and provided that $s(E)$ is well behaved at the threshold, we have that $\tilde{s} \to \text{Im } \tilde{s}$ and hence the conductance reduction is at a maximum. Conversely, as we approach the threshold energy from below, $\kappa_x^{N_{\max}} \to 0$ and again as long as $s(E)$ is reasonably well-behaved in the limit, $\tilde{s} \to \text{Re } \tilde{s}$ and the conductance reduction disappears. A plot of cross section and conductance over a range of energies is shown in Figure 5.7. The Green's function suggests that maximal conductance reduction occurs at a newly opened mode, and this is what is observed as demonstrated in Figure 5.7.

Finally, it should be noted that this is a result of the multiple scattering, as seen in the form of the renormalized scattering strength, and because of this phenomenon is independent of the nature of the scatterer.

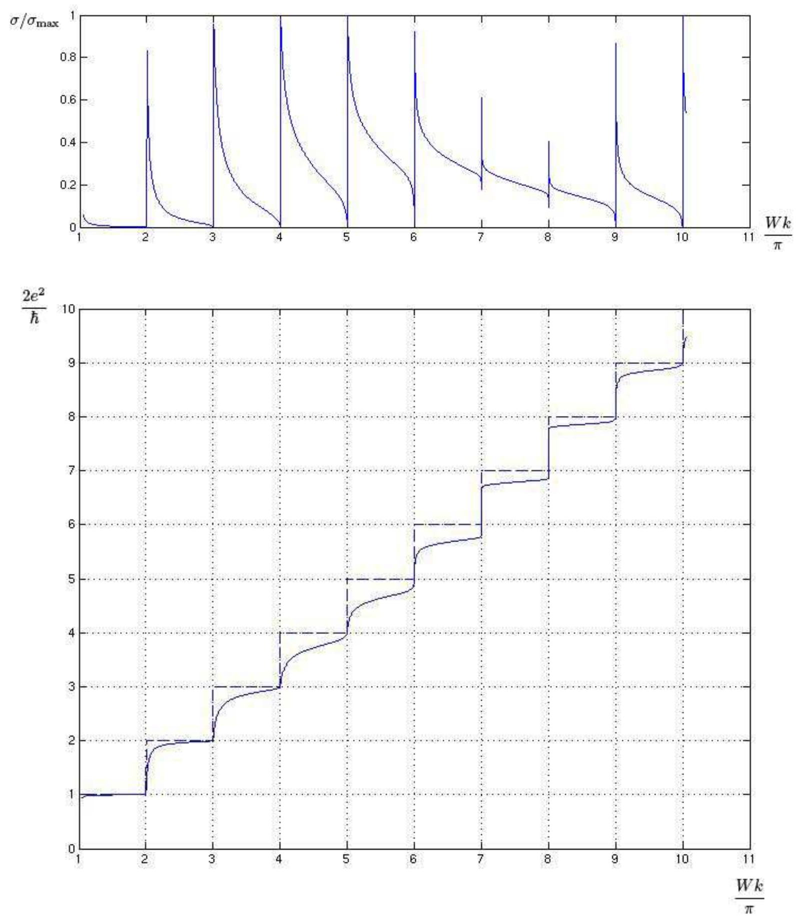

Figure 5.5: Relative cross-section dips and the effect on conductance. *Top:* Plot of $\sigma/\sigma_{\max}$ versus kW ranging from $\pi + .005$ to $10\pi + .05$, just above 1 and 10 allowed modes respectively, with $y_0 = 0.42$, $a = 0.01$ for hard sphere scattering. The cross-section drops to 0 and jumps to 1 at every opening of a new mode; the plot is limited by the number of sample points used in demonstrating this. *Bottom:* Using the formula for conductance (5.50), the reduced conductance caused by the single scatterer (solid line) is plotted against perfect conductance (dashed line) over the same energy range. If an attractive potential had been used instead of a hard sphere, one would have observed conductance dips followed by transparency of the scatterer as discussed above.

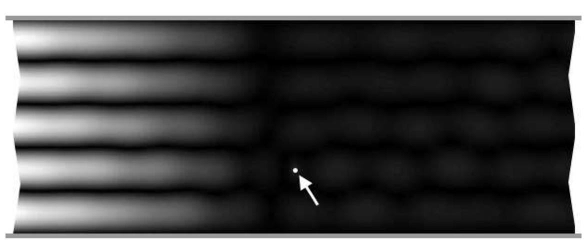

Figure 5.6: Probability density plot of a newly opened mode at $kW = 5\pi + 0.001$ being almost entirely reflected by a single point scatterer with $a = 0.1$ simulating hard sphere scattering. The location of the point scatterer has been highlighted by a dot and arrow. A small but finite amount of transmission exists, but may be difficult to observe in the grayscale image.

5.8 Phase Shifts and s-wave scattering a waveguide

In free-space, partial-wave analysis put the S-matrix in diagonal form which allowed derivation of phase shifts. At low energies, only one phase shift, the s-wave was present. We now extend the idea of a phase shift and the s-wave to scattering in a hard wire.

Because of the use of a point scatterer, it easy to see that one may take linear combinations of the basis wavefunctions ψ_n such that only a single wave scatters. For a point scatterer at $(0, y')$, evaluation of the basis functions $\langle (0, y')|E, m, \pm\rangle$ is a linear map from function space to $\mathbb{C}$ so the image of the map is only of a single dimension. It then becomes a matter of choosing the correct representative basis function, ψ_{img} as to span the image. By careful observation, if we choose (summing over all modes in both directions)

$$\psi_{\text{img}} = \sum_n (\psi_n(0, y')^*)\, \psi_n \tag{5.52}$$

$$= \sum_n \frac{1}{k_x^{(n)}} \chi_n(y')\chi_n(y) e^{ik_x^{(n)} x} \tag{5.53}$$

we see that unless $\psi_n(0, y') = 0$ for all n, ψ_{img} will scatter. Thus we can now choose the remaining basis to be such that scattering occurs if and only if ψ_{img} scatters.

Now we derive a phase-shift analogous to one in free-space. The sum (5.53) occurs over both left- and right-moving modes. For convenience in deriving a phase shift, it will be more convenient to define ψ^+_{img} and ψ^-_{img}, which are defined like ψ_{img} except using only right- or left-moving basis functions.

Taking as our incoming wave $\phi = \psi_{\text{img}}$, with a scatterer at $(0, y')$, we note that

$$\phi(0, y') = \sum_n \frac{1}{k_x^{(n)}} \chi_n(y')\chi_n(y) e^{ik_x^{(n)} x}|_{(0,y')} \tag{5.54}$$

$$= \sum_n \frac{\chi_n(y')^2}{k_x^{(n)}} = 2 \sum_{n=1}^{N_{\max}} \frac{\chi_n(y')^2}{k_x^{(n)}} \tag{5.55}$$

$$= -2 \frac{\text{Im }\tilde{s}}{|\tilde{s}|^2} \left(\frac{\hbar^2}{\mu}\right) \tag{5.56}$$

where in the last step we have used equation (5.41). Using this trick, we write the wavefunction as

$$\psi = \phi + \tilde{s} \left(\frac{2\mu}{\hbar^2}\right) G(x, y, 0, y'; E) \cdot \phi(0, y') \tag{5.57}$$

$$= \phi - 2 \frac{\tilde{s}\text{Im }\tilde{s}}{|\tilde{s}|^2} \left(\frac{\hbar^2}{\mu}\right) \frac{2\mu}{\hbar^2} G(x, y, 0, y'; E) \tag{5.58}$$

$$= \phi - 2 \frac{\tilde{s}\text{Im }\tilde{s}}{|\tilde{s}|^2} \left(-i \sum_{m=1}^{\infty} \chi_m(y)\chi_m(y') \frac{e^{ik_x^{(m)}|x|}}{k_x^{(m)}}\right) \tag{5.59}$$

$$= \phi + \frac{2i\tilde{s}\text{Im }\tilde{s}}{|\tilde{s}|^2} \left(\sum_{m=1}^{\infty} \chi_m(y)\chi_m(y') \frac{e^{ik_x^{(m)}|x|}}{k_x^{(m)}}\right) \tag{5.60}$$

If we take $x \gg 0$, we can neglect the modes that exponentially decay, and equation (5.60) becomes

$$\psi = \left(1 + \frac{2i\tilde{s}\text{Im }\tilde{s}}{|\tilde{s}|^2}\right) \psi^+_{\text{img}} \tag{5.61}$$

while for $x \ll 0$, we have the same for ψ^-_{img}. Because flux is conserved, we therefore conclude that

$$\left(1 + \frac{2i\tilde{s}\text{Im }\tilde{s}}{|\tilde{s}|^2}\right) = e^{2i\delta_0} \tag{5.62}$$

$$\Rightarrow \left(\frac{i\tilde{s}\text{Im }\tilde{s}}{|\tilde{s}|^2}\right) = \frac{e^{2i\delta_0} - 1}{2} \tag{5.63}$$

Using equation (5.46), we have yet another form for the relative cross-section, which passes the consistency check that it varies between 0 and 1:

$$N_{\max}\bar{\sigma} = \left|\frac{e^{2i\delta_0} - 1}{2}\right|^2 \tag{5.64}$$

To compare to freespace, one substitutes (5.63) back into the form of the final wavefunction to get that

$$\psi = \phi_{\text{img}} + \left(\frac{e^{2i\delta_0} - 1}{2}\right) 2 \left(\sum_{m=1}^{\infty} \chi_m(y)\chi_m(y') \frac{e^{ik_x^{(m)}|x|}}{k_x^{(m)}}\right) \tag{5.65}$$

$$\psi = \phi_{\text{img}} + \left(\frac{e^{2i\delta_0} - 1}{2}\right) 4iG(r, r'; E) \tag{5.66}$$

Equations (5.66) and (3.54) are of exactly the same form. For a Dirichlet wire, the Green's function is just an alternating sum of free space Green's functions. The phase shift seen in free space therefore translates in the waveguide to a phase shift created by the original scatterer superimposed with its images. Asymptotically, one thus observes a "hall of mirrors" effect in the waveguide. As in free space, we also see that specifying a phase shift is equivalent to also defining the cross section generated by the scatterer.

5.9 Optical Theorem for a Waveguide

From (5.42), one may suspect that there is an optical theorem equivalent that may be derived for a waveguide. Because the geometry differs from that of two-dimeionsal free-space and a one-dimensional problem, we expect such a relation to be similar to both such optical theorem relations. We begin with the Lippman-Schwinger equation and write the scattering amplitude in terms of a unit flux-normalized basis.

$$\psi = \phi + \frac{2\mu}{\hbar^2} GV\psi \tag{5.67}$$

$$= \phi + \frac{2\mu}{\hbar^2}(-i) \sum_{n=1}^{\infty} \int d^2x' \chi_n(y)\chi_n(y') \frac{e^{ik_x^{(n)}|x-x'|}}{2k_x^{(n)}} V(x')\psi(x') \tag{5.68}$$

Asymptotically, we can neglect the modes past $N_{\max}$, the maximum quantum number for the transverse modes and take $e^{ik_x^{(n)}|x-x'|} = e^{\pm ik_x^{(n)}(x-x')}$ according to whether we're evaluating a point at $x \gg 0$ or $x \ll 0$.

This allows us to rewrite (5.68) as

$$\begin{aligned}
\psi &\rightarrow \phi + \frac{\mu}{\hbar^2}(-i)\sum_{n=1}^{\infty}\chi_n(y)\frac{e^{\pm ik_x^{(n)}x}}{\sqrt{k_x^{(n)}}}\int d^2x'\chi_n(y')\frac{e^{\mp ik_x^{(n)}x'}}{\sqrt{k_x^{(n)}}}V(x')\psi(x') && (5.69)\\
&= \phi + \sum_{n=1}^{N_{\text{max}}}\chi_n(y)\frac{e^{\pm ik_x^{(n)}x}}{\sqrt{k_x^{(n)}}}\left(\frac{\mu}{\hbar^2}(-i)\langle n^{\pm}|V|\psi\rangle\right) && (5.70)\\
&= \phi + \sum_{n=1}^{N_{\text{max}}}\chi_n(y)\frac{e^{\pm ik_x^{(n)}x}}{\sqrt{k_x^{(n)}}}\left(\frac{\mu}{\hbar^2}(-i)\langle n^{\pm}|T|\phi\rangle\right) && (5.71)\\
&\equiv \phi + \sum_{n=1}^{N_{\text{max}}}\langle x|n^{\pm}\rangle\left(\frac{\mu}{\hbar^2}(-i)\langle n^{\pm}|T|\phi\rangle\right) && (5.72)
\end{aligned}$$

where we have kept the $\pm$ to remind us that ψ require a different integral depending on whether we are asymptotically to the right or left of a scattering potential's range. If we let $\phi = |m\rangle$, then we get that

$$\begin{aligned}
\psi &= \langle x|m\rangle + \sum_{n=1}^{N_{\text{max}}}\langle x|n^{\pm}\rangle\left(\frac{\mu}{\hbar^2}(-i)\langle n^{\pm}|T|m\rangle\right) && (5.73)\\
&\equiv \phi + \sum_{n=1}^{N_{\text{max}}}\langle x|n^{\pm}\rangle g_{nm}^{\pm} && (5.74)
\end{aligned}$$

where we have used g's instead of f's to stand for the scattering amplitudes to note that our basis is normalized to unit flux. But this means that

$$\langle n|S|m\rangle = \delta_{nm} + g_{nm} \tag{5.75}$$

where the $n, \pm$ index has been replaced just by n. Applying the unitary condition of the S matrix, we then get that

$$\sum_n |S_{mn}|^2 = 1 \tag{5.76}$$

$$\Rightarrow |1 + g_{mn}|^2 + \sum_{n\neq m}|g_{mn}|^2 = 1 \tag{5.77}$$

$$\Rightarrow 2\text{Re } g_{mm} = -\sum_n |g_{mn}|^2 \tag{5.78}$$

Now we want to relate this to the cross-section of the wire. Since our basis function is normalized to unit flux through the wire, we just need to calculate the total scattered flux to get the cross-section. This is found by calculating the flux of

$$\psi_{\text{scat}} = \sum_{n=1}^{N_{\text{max}}}\langle x|n^{\pm}\rangle g_{nm}^{\pm} \tag{5.79}$$

at $x \gg 0$ and $x \ll 0$. However, since again we're in a basis normalized to unit flux, this just becomes $\sum_n |g_{nm}|^2$ so that

$$\sigma_m = \sum_n |g_{nm}|^2 \tag{5.80}$$

where the sum runs over all modes. Our optical theorem, derived in a flux-normalized basis, is then

$$\text{Re } g_{mm} = -\frac{1}{2}\sigma_m \tag{5.81}$$

For the case of a wire with periodic boundary conditions instead of the hard walls that we have been working with, the $m = 0$ mode looks the most like the free space case. Applying (5.81) to

$$\phi(x,y) = \frac{e^{ik_x^{(0)}}}{k_x^{(0)}} \tag{5.82}$$

then, we can show quite easily that this reduces into the free space optical theorem. From (5.34), we have that the real part of the forward scattering amplitude is

$$\begin{aligned} R_{00} &= \left(\frac{-i\mu\tilde{s}}{\hbar^2}\frac{\chi_0(y')\chi_0(y')}{\sqrt{k_x^{(0)}k_x^{(0)}}}\right) && (5.83)\\ &= \left(\frac{-i\mu\tilde{s}}{\hbar^2}\frac{1}{k_x^{(0)}}\right) && (5.84)\\ \Rightarrow \text{Re } R_{00} &= \frac{\mu}{\hbar^2}\frac{1}{k}\text{Im } \tilde{s} && (5.85)\\ \Rightarrow \sigma &= \frac{2\mu}{\hbar^2}\frac{1}{k}(-\text{Im } \tilde{s}) && (5.86) \end{aligned}$$

where $k_x^{(0)} = k$ since for $m = 0$, $k_y = 0$. In the limit as $W \to \infty$, renormalization must become less important so $\tilde{s} \to s$ and we may apply the free space unitarity condition (4.20) for a point scatterer to get

$$\sigma \to \left(\frac{\mu}{\hbar^2}\right)\frac{1}{k}|s|^2 \tag{5.87}$$

which for $\phi(0) = 1$ in this case is exactly the free space cross section (4.13). Alternately, we could have substituted the waveguide unitarity constraint (5.41), taken the limit, and arrived at the same answer.

In summary, as was suggested at the beginning of this section, this optical theroem looks like the same equation in one dimension [3]. However, the relation holds in a basis with unit flux normalization so that the two-dimensional aspect of the problem has modified what me might consider a one-dimensional problem.

Chapter 6

Conclusion

As we have demonstrated, it is not only possible to model s-wave scattering in a waveguide through the use of t-matrices and the Green's function, but through the use of renormalized t-matrix theory, multiple scattering, and the method of images, it is possible to understand many scattering phenomena of waveguides in terms of free space scattering. Examining a scatterer's cross section as a result of its placement in the waveguide, one sees that many features in its cross section can be understood in terms of multiple scattering of a scatterer and its images. Similarly, renormalized scattering theory is able to account for the threshold behavior of scattering cross sections.

There are several directions to take future work. Our discussion here of the interaction of the wavefunction, scatterer, and its images has only begun to explore scattering phenomena due to multiple scattering in the wire. As our work has considered only s-wave scatterers and their analogues in the wire, inclusion of higher partial waves is the next logical step in modeling higher energies. A model for inclusion of higher partial waves using point scatterers is detailed in [13] and could be applied from free space to the wire using renormalized t-matrices.

Another interesting observation in Figure 5.4 is that the number of resonant peaks appears to be the number of allowed modes plus the two p-wave resonances at the edges. Understanding this phenomenon may lead to a better overall understanding of the interaction between wave, scatterer, and images.

Having treated the case of a single scatterer in a waveguide, calculations of the statistical properties of collections of scatterers may be of interest in studying localization and disorder. Of greater experimental relevance, studying scatterer ensembles within waveguides may be of interest in understanding coherence length with potential applications in atomic interferometry and other quantum devices.

Appendix A

Eigenfunction Expansion of the Green's Function for a Dirichlet wire

One of the most used methods is via eigenfunction expansion using the expression

$$1 = \int df |E,f\rangle\langle E,f| \tag{A.1}$$

$$\Rightarrow G(x,x';E) = \int df \frac{\langle x|E,f\rangle\langle E,f|x'\rangle}{E - H_0 + i\epsilon} \tag{A.2}$$

Here we have assumed indexing of eigenstates at energy E by the continuous property f though using a sum over a discrete one would also suffice.

We now follow the derivation in [18] for calculating the Green's function of a separable system. In two-dimensional systems in which one dimension is free, we have a basis of the form $|m\rangle \otimes |k_x^{(m)}\rangle$ so that our eigenfunction expansion becomes

$$\frac{\hat{1}}{E - H_0^{(x)} - H_0^{(y)} + i\epsilon} = \frac{\sum_m \int dk |m\rangle \otimes |k_x^{(m)}\rangle\langle m| \otimes \langle k_x^{(m)}|}{E - E_x - E_y + i\epsilon} \tag{A.3}$$

$$= \sum_m |m\rangle\langle m| \otimes \frac{\int dk |k_x^{(m)}\rangle\langle k_x^{(m)}|}{(E - E_y) - E_x + i\epsilon} \tag{A.4}$$

We now recognize the inner integral as just the one-dimensional Green's function for a free particle at energy $E - E_y$. The Green's function for our system is then

$$\langle x|G|x'\rangle = \sum_m \langle x|m\rangle\langle m|x'\rangle G_0(x,x';E - E_y) \tag{A.5}$$

For a Dirichlet wire, this is just

$$G(x,x') = \sum_{m=1}^{\infty} \chi_m(y)\chi_m(y')[\frac{-ie^{ik_x^{(m)}|x-x'|}}{2k_x^{(m)}}] \tag{A.6}$$

where $\chi_m(y) = \sqrt{\frac{2}{W}}\sin(\frac{m\pi}{W}y)$, the usual eigenfunction for a particle in a box.

Appendix B

Acceleration of Green's Function Convergence

We wish to consider a more rapidly converging form of the Green's function:

$$G_w(\vec{r},\vec{r}_0;k) = [G_w(\vec{r},\vec{r}_0;k) - \alpha G_w(\vec{r},\vec{r}_0;0)] + \alpha G_w(\vec{r},\vec{r}_0;0) \tag{B.1}$$

where we shall determine α, the constant of proportionality (this procedure is called Kummer's method of convergence acceleration). We use equation (A.6) with $E = 0$ so that $k_x^{(m)} = ik_y^{(m)}$.

$$\begin{aligned}
G_w(\vec{r},\vec{r}_0;0) &= -\frac{1}{2}\sum_{m=1}^{\infty}\chi_m(y)\chi_m(y_0)\frac{e^{-k_y^{(m)}|x-x_0|}}{k_y^{(m)}} \\
&= -\frac{1}{2}\sum_{m=1}^{\infty}\frac{W}{m\pi}\chi_m(y)\chi_m(y_0)e^{-\frac{m\pi}{W}|x-x_0|} \\
&= -\frac{1}{2\pi}\sum_{m=1}^{\infty}\frac{W}{m}\times\frac{2}{W}\sin\left(\frac{m\pi y}{W}\right)\sin\left(\frac{m\pi y_0}{W}\right)e^{-\frac{m\pi}{W}|x-x_0|} \\
&= \frac{1}{2\pi}\sum_{m=1}^{\infty}\left[\cos\left(\frac{m\pi(y+y_0)}{W}\right) - \cos\left(\frac{m\pi(y-y_0)}{W}\right)\right]e^{-\frac{m\pi}{W}|x-x_0|} \\
&= \frac{1}{2\pi}\mathrm{Re}\sum_{m=1}^{\infty}e^{-\frac{m\pi}{W}|x-x_0|}\left[e^{\frac{im\pi(y+y_0)}{W}} - e^{\frac{im\pi(y-y_0)}{W}}\right] \\
&= \frac{1}{2\pi}\mathrm{Re}\sum_{m=1}^{\infty}\left(\frac{Z_+^m}{m} - \frac{Z_-^m}{m}\right)
\end{aligned}$$

where

$$Z_\pm \equiv e^{-\frac{\pi}{W}|x-x_0|}e^{\frac{i\pi(y\pm y_0)}{W}} \tag{B.2}$$

Using the identities

$$\sum_{m=1}^{\infty}\frac{Z^m}{m} = -\ln(1-Z) \tag{B.3}$$

and

$$\mathrm{Re}\ln Z = \ln|Z| \tag{B.4}$$

we find

$$
\begin{aligned}
G_w(\vec{r},\vec{r}_0;0) &= \frac{1}{2\pi}\ln\left|\frac{1-Z_-}{1-Z_+}\right| \\
&= \frac{1}{4\pi}\ln\left(\left|\frac{1-Z_-}{1-Z_+}\right|^2\right) \\
&= \frac{1}{4\pi}\ln\left|\frac{e^{\frac{\pi}{W}|x-x_0|}-e^{\frac{i\pi}{W}(y-y_0)}}{e^{\frac{\pi}{W}|x-x_0|}-e^{\frac{i\pi}{W}(y+y_0)}}\right|^2 \\
&= \frac{1}{4\pi}\ln\frac{\left(e^{\frac{\pi}{W}|x-x_0|}-e^{\frac{i\pi}{W}(y-y_0)}\right)\left(e^{\frac{\pi}{W}|x-x_0|}-e^{-\frac{i\pi}{W}(y-y_0)}\right)}{\left(e^{\frac{\pi}{W}|x-x_0|}-e^{\frac{i\pi}{W}(y+y_0)}\right)\left(e^{\frac{\pi}{W}|x-x_0|}-e^{-\frac{i\pi}{W}(y+y_0)}\right)} \\
&= \frac{1}{4\pi}\ln\frac{\cos\left[\frac{\pi}{W}(y-y_0)\right]-\cosh\left[\frac{\pi}{W}(x-x_0)\right]}{\cos\left[\frac{\pi}{W}(y+y_0)\right]-\cosh\left[\frac{\pi}{W}(x-x_0)\right]}
\end{aligned}
\tag{B.5}
$$

The singularity of the Green's function arises from a logarithmic singularity in the Hankel term at the source. Near the scatterer, the contribution from this term becomes

$$
\begin{aligned}
\lim_{r\to r_0} G_0(r,r_0;k) &= -\frac{i}{4}\lim_{\vec{r}\to\vec{r}_0} H_0(k\,|\vec{r}-\vec{r}_0|) \\
&= -\frac{i}{4}+\frac{1}{2\pi}\ln\left(\frac{k}{2}\,|\vec{r}-\vec{r}_0|\right)+\frac{1}{2\pi}\gamma \\
&= -\frac{i}{4}+\frac{\gamma-\ln 2}{2\pi}+\frac{1}{2\pi}\ln k+\frac{1}{2\pi}\ln|r-r_0|
\end{aligned}
\tag{B.6}
$$

while from (B.5), we find that the limiting behavior of the static Green's function is

$$
\begin{aligned}
\lim_{\vec{r}\to\vec{r}_0} G_w(\vec{r},\vec{r}_0;0) &= \frac{1}{2\pi}\left[\ln\left(\frac{\pi}{2W}|\vec{r}-\vec{r}_0|\right)-\ln(1-\cos\left(\frac{2\pi y_0}{W}\right))\right] \\
&= \frac{1}{2\pi}[\ln\frac{\pi}{2W}-\ln(1-\cos(\frac{2\pi y_0}{W})]+\frac{1}{2\pi}\ln|r-r_0|
\end{aligned}
\tag{B.7}
$$

where γ is the Euler-Mascheroni constant. We see that in order to cancel the logarithmic singularity in Green's function, we require simply that

$$\alpha = 1 \tag{B.8}$$

so that

$$\lim_{\vec{r}\to\vec{r}_0}\left[G_0(\vec{r},\vec{r}_0;k)-G_w(\vec{r},\vec{r}_0;0)\right] = \frac{1}{2\pi}\ln\left[\frac{kW}{\pi}(1-\cos(\frac{2\pi y_0}{W})\right]-\frac{i}{4}+\frac{\gamma}{2\pi} \tag{B.9}$$

Our final form for the Green's function, using equation (B.5) through (B.8) is

$$
\begin{aligned}
G_w(\vec{r},\vec{r}_0;k) = -\frac{i}{2}\sum_{m=1}^{\infty}\chi_m(y)\chi_m(y_0)(\frac{1}{k_x^{(m)}}e^{ik_x^{(m)}|x-x_0|}+\frac{iW}{m\pi}e^{-\frac{m\pi}{W}|x-x_0|}) \\
-\frac{1}{4\pi}\ln\frac{\cos\left[\frac{\pi}{W}(y-y_0)\right]-\cosh\left[\frac{\pi}{W}(x-x_0)\right]}{\cos\left[-\frac{\pi}{W}(y+y_0)\right]-\cosh\left[\frac{\pi}{W}(x--x_0)\right]}
\end{aligned}
\tag{B.10}
$$

which can be shown to converge uniformly [18]. This is of further use in that it allows us to obtain another form of the renormalization constant λ from equation (5.20)

$$\lambda = \frac{-i}{4}\sum_{m\neq 0, m=-\infty}^{\infty}(-1)^m H_0(k|\vec{r}_n-\vec{r}_0|) \tag{B.11}$$

$$
\begin{aligned}
\Rightarrow \lambda &= \lim_{\vec{r}\to\vec{r}_0} \left(G_w(\vec{r},\vec{r}_0;k) - G_0(\vec{r},\vec{r}_0;k)\right) \\
&= \lim_{\vec{r}\to\vec{r}_0} \left(G_w(\vec{r},\vec{r}_0;k) - G_w(\vec{r},\vec{r}_0;0)\right) + \left(G_w(r,r_0;0) - G_0(r,r_0;k)\right) \\
&= \frac{-i}{2}\sum_{m=1}^{\infty}\left(\frac{1}{k_x^{(m)}} + \frac{iW}{m\pi}\right)\chi_m(y_0)^2 \\
&\quad -\frac{1}{2\pi}\ln\left[\frac{kW}{\pi}(1-\cos(\frac{2\pi y_0}{d})\right] - \frac{i}{4} + \frac{\gamma}{2\pi}
\end{aligned}
\tag{B.12}
$$

Appendix C

Scatterer Renormalization via Free Space Multiple Scattering in a Hard Wire

Start as before with N point-scatterers in a wire, then reflect them up and down in the channel to $\pm\infty$ to get free space. Dealing with an anti-symmetric solution to this problem, the boundary conditions will be satisfied for the Dirichlet-boundary wire.

The equation for the final wavefunction is the incoming wavefunction plus the contribution from the point scatterers. The contribution each point-scatterer contributes at a point is equal to the incoming amplitude at the k-th location multiplied by the scatterer strength s^k and propagated by the Green's function centered at the k-th location. This is expressed below:

$$\psi(r) = \phi(r) + \sum_k s_k \cdot G_0(r, r_k) \cdot \alpha_k(r_k) \tag{C.1}$$

We now introduce some bookkeeping to rewrite the sum over scatterer locations. Index the scatterer locations in the wire (the real locations) by the upper index $k = \{1 \ldots N\}$. Index the particular wire image in which they are located by the lower index $j \in \mathbb{Z}$. All For example r_l^m represents an image of the l-th scatterer from the original wire in the m-th wire image. To avoid confusion with taking powers, we note that all manipulations that will occur using this notation will NOT involve multiplying doubly-indexed values of the same type together until we derive matrix equations to do away with this notation.

The sum (C.1) may be rewritten as

$$\psi(r) = \phi(r) + \sum_{k=1}^{N} \sum_{j=-\infty}^{\infty} s^k \cdot G_0(r, r_j^k) \cdot \alpha_j^k(r_j^k) \tag{C.2}$$

Applying anti-symmetry across the wires, we know that $\alpha_j^k(r_j^k) = (-1)^j \alpha_0^k(r_0^k)$. Therefore solving for the amplitude hitting the $k - th$ scatterer in the zeroth channel will solve the scattering problem for us. The amplitude hitting the k-th wire in the zeroth channel can be written as the incoming wavefunction plus the amplitude coming from all of the other scatterers (but not itself):

$$\alpha_0^k(r_0^k) = \phi(r_0^k) + \sum_{j\neq 0, j=-\infty}^{\infty} s^k G_0(r_0^k, r_j^k) \alpha_j^k(r_j^k) + \sum_{p\neq k}^{N} \sum_{j=-\infty}^{\infty} s^p G_0(r_0^k, r_j^p) \alpha_j^p(r_j^p) \tag{C.3}$$

We'll now abbreviate notation to shorten things:

$$\alpha_0^k = \phi_0^k + \sum_{j\neq 0, j=-\infty}^{\infty} s^k G_{0,j}^{k\leftarrow k} \alpha_j^k + \sum_{p\neq k}^{N} \sum_{j=-\infty}^{\infty} s^p G_{0,j}^{k\leftarrow p} \alpha_j^p \tag{C.4}$$

Applying anti-symmetry yields

$$\alpha_0^k = \phi_0^k + \sum_{j\neq 0, j=-\infty}^{\infty} s^k G_{0,j}^{k\leftarrow k}(-1)^j \alpha_0^k + \sum_{p\neq k}^{N} \sum_{j=-\infty}^{\infty} s^p G_{0,j}^{k\leftarrow p}(-1)^j \alpha_0^p \tag{C.5}$$

This leads us to a matrix equation. We define λ_{kp} as follows:

$$\lambda_{kp} = \begin{cases} \sum_{j=-\infty}^{\infty} s^p G_{0j}^{k\leftarrow p}(-1)^j & \text{if } k \neq p \\ \sum_{j\neq 0, j=-\infty}^{\infty} s^k G_{0,j}^{k\leftarrow k}(-1)^j & \text{if } k = p \end{cases} \tag{C.6}$$

We then define the matrix $\mathbf{S_{ij}} = \mathbf{s^i} \cdot \delta_{\mathbf{ij}}$, a diagonal matrix with the s^i on the i-th diagonal. Defining the matrices $\Lambda \equiv \lambda_{ij}$, $\boldsymbol{\alpha}_{1j} \equiv \alpha_0^j$, and $\Phi_{1j} = \phi_0^j$, we get that

$$\alpha = \Phi + \Lambda \mathbf{S} \boldsymbol{\alpha} \tag{C.7}$$

$$\Rightarrow \boldsymbol{\alpha} = (I - \Lambda \mathbf{S})^{\mathbf{-1}} \boldsymbol{\Phi} \tag{C.8}$$

This tells us that for N scatterers in the wire, we must calculate N^2 infinite sums and invert an N by N matrix to solve the problem. To recap, the overall wavefunction is then

$$\psi(r) = \phi(r) + \sum_{k=1}^{N} \sum_{j=-\infty}^{\infty} G_0(r, r_j^k)(-1)^j \{s^k [[I - \Lambda \mathbf{S}]^{\mathbf{-1}} \boldsymbol{\Phi}]_{\mathbf{k}}\} \tag{C.9}$$

To put things in a form similar to the one-scatterer case, we have

$$\psi(r) = \phi(r) + \mathbf{G_V}[\mathbf{S}[\mathbf{I} - \boldsymbol{\Lambda}\mathbf{S}]^{\mathbf{-1}} \boldsymbol{\Phi}] \tag{C.10}$$

where $(\mathbf{G_V})_{\mathbf{j}} = \mathbf{G_V}(\mathbf{r}, \mathbf{r^k})$, the Green's function for the wire centered around the kth scatterer.

Appendix D

Bessel Functions

D.1 Definition

Bessel functions of order α are defined as solutions y(x) to the differential equation

$$x^2\frac{d^2y}{dx^2} + x\frac{dy}{dx} + (x^2 - \alpha^2)y = 0 \tag{D.1}$$

For a fixed α, this is a second order differential equation and thus there are two linearly independent solutions. It turns out that one solution, defined as $J_\alpha(x)$ (the First Kind) is finite at the origin while the other $Y_\alpha(x)$ (the Second Kind) is singular at the origin.

Away from the origin, the Hankel functions

$$H_\alpha^{(1)} = J_\alpha + iY_\alpha \tag{D.2}$$

$$H_\alpha^{(2)} = J_\alpha - iY_\alpha \tag{D.3}$$

are also valid solutions to equation (D.1).

D.2 Asymptotic Behavior

For $x \gg 1$,

$$J_\alpha(x) \rightarrow \sqrt{\frac{2}{\pi x}}\cos(x - \frac{\alpha\pi}{2} - \frac{\pi}{4}) \tag{D.4}$$

$$Y_\alpha(x) \rightarrow \sqrt{\frac{2}{\pi x}}\sin(x - \frac{\alpha\pi}{2} - \frac{\pi}{4}) \tag{D.5}$$

$$\Rightarrow H_\alpha^{(1)}(x) \rightarrow \sqrt{\frac{2}{\pi x}}e^{i(x - \frac{\alpha\pi}{2} - \frac{\pi}{4})} \tag{D.6}$$

$$\Rightarrow H_\alpha^{(2)}(x) \rightarrow \sqrt{\frac{2}{\pi x}}e^{-i(x - \frac{\alpha\pi}{2} - \frac{\pi}{4})} \tag{D.7}$$

For $x \ll 1$ and $l \in \mathbb{Z}$,

$$J_l(kr) \rightarrow \frac{1}{l!}\left(\frac{kr}{2}\right)^l \tag{D.8}$$

$$Y_l(kr) \rightarrow \begin{cases} \frac{2}{\pi}\{\ln(\frac{1}{2}kr) + \gamma\} & l = 0, \\ -\frac{(l-1)!}{\pi}\left(\frac{2}{kr}\right)^l & l > 0. \end{cases} \tag{D.9}$$

$$H_0^{(1)}(kr) = 1 + \frac{2i}{\pi}\{\ln(\frac{1}{2}kr) + \gamma\} \tag{D.10}$$

$$= 1 + \frac{2i}{\pi}(\ln\frac{k}{2} + \gamma) + i\ln r \tag{D.11}$$

D.3 Integral for Normalization

$$\int_0^\infty xJ_\alpha(mx)J_\alpha(nx)dx = \frac{1}{m}\delta(m-n) \tag{D.12}$$

Bibliography

[1] Abramowitz and Stegan. *Handbook of Mathematical Functions with Formulas, Graphs, and Mathematical Tables, 9th printing.* New York: Dover, p. 16, 1972.

[2] S. Albeverio, F. Geszetsky, R. Høegh-Krohn and H. Holden. *Solvable Models in Quantum Mechanics* Springer-Verlag, Berlin, 1998.

[3] Vania E. Barlette, Marcelo M. Leite, and Sadhan K. Adhikari. Integral equations of scattering in one dimension. *American Journal of Physics* **69** (2001) 1010-1013.

[4] Supriyo Datta. *Electronic transport in mesoscopic systems.* Cambridge; New York: Cambridge University Press, 1995.

[5] Yick Stella Chan. *Theories and Applications of Multiple Scattering S-wave Scatterers.* PhD Thesis, Harvard University, 1997.

[6] C.S. Chu and R.S. Sorbello. Effect of Impurities on the Quantized Conductance of Narrow Channels. *Physics Review B*, **40**, 5941 (1989).

[7] P. Exner, P. Seba. Point interactions in two and three dimensions as models of small scatterers. *Physics Letters A* **222**, 1-4 (1996).

[8] J. Faist, P. Gueret, and H. Rothuizen. Possible Observation of Impurity Effects on Conductance Quantization. *Physics Review B* **42** (5), 1990.

[9] E. Granot. Universal conductance reduction in a quantum wire. *Europhysics Letters*, **68** (6), (2004).

[10] David J. Griffiths *Introduction to Quantum Mechanics.* Prentice Hall, New Jersey, 1995.

[11] E.J. Heller, M.F. Crommie, C.P. Lutz, and D.M. Eigler. Scattering and absorption of surface electron waves in quantum corrals. *Nature* **369** 464 (1994).

[12] E.J. Heller. Quantum Proximity Resonances. *Physics Review Letters* **77** 20, 4122-5 (1996).

[13] J.S. Hersch. *Scattering Resonances in the Extreme Quantum Limit.* PhD Thesis, Harvard University, 1999.

[14] Rubin H. Landau *Quantum Mechanics II - A Second Course in Quantum Theory.* John Wiley & Sons, Inc., 1990.

[15] H. Lee, H. Hsu, and L.E. Reichl. Modeling conduction in electron waveguides with finite-range impurities. *Physics Review B* **71** 045307 (2005).

[16] W. Liang, M. Bockrath, D. Bozovic, J.H. Hafne, M. Tinkham, H. Park. Fabry-Perot Interference in a Nanotube Electron Waveguide. *Nature* **411** 665 (2001).

[17] C. Linton and P. Martin, Semi-Infinite Arrays of Isotropic Point Scatterers. A Unified Approach. *SIAM: Journal of Applied Mathematics* **64**, 1035 (2004).

[18] Adam Lupu-Sax. *Quantum Scattering Theory and Applications: a thesis presented by Adam Lupu-Sax.* PhD Thesis, Harvard University, 1998.

[19] M.G.E. da Luz, A. Lupu Sax, and E.J. Heller. Quantum Scattering from Arbitrary Boundaries. *Physics Review E* **56**, 2496 (1997).

[20] M.G. Moore, T. Bergeman, and M. Olshanii. Scattering in tight atom waveguides. *Journal de Physique IV France* **1** (2004).

[21] M. Olshanii. Atomic Scattering in the Presence of an External Confinement and a Gas of Impenetrable Bosons. *Physics Review Letters* **81** 938 (1998).

[22] Jun John Sakurai *Modern Quantum Mechanics.* Addison-Wesley Publishing Company, 1994.

[23] R. Shankar *Principles of Quantum Mechanics, 2nd ed.* Plenum Press, New York, 1994.

[24] A.D. Stone and A. Szafer. What is measured when you measure resistance? The Landauer formula revisited. *IBM Journal of Research and Development* **32** (1998).

[25] John R. Taylor *Scattering Theory: The Quantum Theory of Nonrelativistic Collisions.* John Wiley & Sons, Inc., 1972.

[26] M.A. Topinka, B.J. LeRoy, R.M. Westervelt, S.E.J. Shaw, R. Fleischmann, E.J. Heller, K.D. Maranowski, A.C. Gossard. Coherent Branched Flow In a Two-Dimensional Electron Gas. *Nature* **410** 283 (2001).

[27] B.J. van Wees, H. van Houten, C.W.J. Beenakker, J.G. Williamson, L.P. Kouwenhoven, D. van der Marel, and C.T. Foxon. Quantized Conductance of Point Contacts in a Two-dimensional Electron Gas. *Physics Review Letters* **60** 848 (1988).